Supporting Information

Organic & Biomolecular Chemistry

Molecular engineering of logic gate types by module rearrangement in 'Pourbaix Sensors': the effect of excited-state electric fields

Jake C. Spiteri,[a] Sergey A. Denisov,[b] Gediminas Jonusauskas,[c] Sylwia Klejna,[d] Konrad Szaciłowski,[d] Nathan D. McClenaghan[b] and David C. Magri[a]*

[a]Department of Chemistry, Faculty of Science, University of Malta, Msida, MSD 2080, Malta. phone: 356 2340 2276, E-mail: david.magri@um.edu.mt

[b]Institut des Sciences Moléculaires, CNRS UMR 5255, University of Bordeaux, 33405 Talence, France, E-mail: nathan.mcclenaghan@u-bordeaux.fr

[c]Laboratoire Ondes et Matière d'Aquitaine, CNRS UMR 5798, University of Bordeaux, 33405 Talence, France, E-mail: gediminas.jonusauskas@u-bordeaux.fr

[d]AGH University of Science and Technology, Academic Centre for Materials and Nanotechnology, Mickiewicza 30,30-059 Kraków, Poland, E-mail:szacilow@agh.edu.pl

Table of Contents

Experimental

Chemicals

1-Methylpiperazine (98+%, Alfa Aesar), 1,4-dioxane (99+%, Sigma-Aldrich), 1,2-dichloroethane (> 99%, Fisher Chemicals), 4-(2-aminoethyl)morpholine (99%, Acros Organics), 4-bromo-1,8-naphthalic anhydride (95%, Sigma-Aldrich), acetone (GPR Grade, LEVO Laboratory Services), chloroform (HPLC Grade, Sigma-Aldrich), chloroform-*d* (99.8 atom %D, Sigma-Aldrich), dichloromethane (HPLC Grade, Sigma-Aldrich), diethyl ether (HPLC Grade, Sigma-Aldrich), ethanol (HPLC Grade, Fisher Chemicals), ethyl acetate (HPLC Grade, Sigma-Aldrich), ferrocenecarboxaldehyde (98%, Acros Organics), glacial acetic acid (> 99.9%, Carlo Erba), hexane 40-60 °C (HPLC Grade, Sigma-Aldrich), hydroxylamine (50 wt % in H_2O, Sigma-Aldrich), iron(III) sulfate pentahydrate (97%, Sigma-Aldrich), lithium aluminium hydride (97%, Alfa Aesar), methanesulfonic acid (≥ 99.5%, Sigma-Aldrich), methanol (HPLC Grade, Carlo Erba), *N*,*N*-dimethylethylenediamine (≥ 98.0%, Sigma-Aldrich), piperazine (99%, Alfa Aesar), pyridine (≥ 99.5%, Merck), sodium triacetoxyborohydride (95%, Sigma-Aldrich), tetrabutylammonium hydroxide (25 wt % in H_2O, Sigma-Aldrich), tetrahydrofuran (HPLC Grade, Sigma-Aldrich), triethylamine (HPLC Grade, Fisher Chemicals). 4 Å molecular sieves (Roth) were activated in a furnace at 350 °C for 72 hours before use and stored in an oven at 120 °C. Silica gel 60 (70-230 mesh, Fluka Analytical) and silica on TLC aluminium foils (silica gel matrix with fluorescent indicator 254 nm, Fluka Analytical) were used for column and thin-layer chromatography, respectively.

Instrumentation

^{1}H and ^{13}C NMR spectra were recorded on a Bruker Avance III HD NMR spectrometer equipped with an Ascend 500 11.75 Tesla Superconducting Magnet, operating at a frequency of 500.13 MHz for ^{1}H NMR and 125.76 MHz for ^{13}C NMR and with a multinuclear 5 mm PABBO Probe. Data were acquired and processed via Topspin Software, ver. 3.2. Chemical shifts for ^{1}H NMR were recorded in ppm downfield from TMS set at $\delta = 0.00$ ppm and ^{13}C NMR spectra were referenced to the solvent triplet signal of $CDCl_3$ at $\delta = 77.00$ ppm. Infra-red spectra were recorded on a Shimadzu IR-

affinity 1 FT-IR spectrometer calibrated against polystyrene at 1602 cm^{-1} as KBr disks. Electrospray time-of-flight (ES-TOF) spectra were performed on a Waters LC Premier instrument. pH measurements were recorded with a Hanna Instruments pH 210 microprocessor meter with a HI 1131 electrode calibrated at pH 4.00 and pH 7.00.

UV-visible absorption spectra were recorded on a Jasco V-650 spectrophotometer connected to a desktop computer. The instrumentation parameters were set to medium response, bandwidth of 2 nm and scan speed of 200 nm min^{-1}. Samples were scanned over the range of 350-600 nm. All spectra were background corrected for the solvent by scanning the appropriate blank solvent prior to beginning the experiments. Fluorimetric studies were conducted using a Jasco FP-8300 spectrophotometer with a 10 mm path length quartz cuvette. The excitation and emission slits were set at 2.5 and 5.0 nm, respectively. The emission range was 400-650 nm, unless otherwise stated. The time-resolved luminescence and subpicosecond time scale set-ups were previously described.[S1]

Syntheses

Synthesis of Ferrocenylmethylamine

The synthesis of ferrocenylmethylamine was based on published procedures.[S2,S3] See Scheme S1. Ferrocenecarboxaldehyde (1.06 g, 4.95 mmol) was dissolved in 30 mL of ethanol and with hydroxylamine (0.652 g, 19.8 mmol). The mixture was stirred and refluxed for 4 hours at 90 °C. The crude oxime was hydrolysed with 50 mL water and extracted with dichloromethane (3×30 mL). The organic phase was dried over anhydrous $MgSO_4$ and filtered. The solvent was removed under vacuum by rotary evaporator to give an orange solid. The oxime was dissolved in 20 mL of dry THF and reduced to the amine by $LiAlH_4$ (0.756 g, 19.9 mmol) under an inert nitrogen atmosphere. The reaction mixture was stirred and refluxed at 80 °C for 24 hours. Excess reducing agent was reacted with water and the amine extracted in diethyl ether (3×30 mL). The organic phase was dried using $MgSO_4$, filtered and excess solvent removed under vacuum. The final product was purified by column chromatography eluted with ethyl acetate. The amine was the last band and its collection was aided by the addition of 100:1 (*v*/*v*) ethyl

acetate/triethylamine. The solvent was removed by rotary evaporator to give an orange oil in 41% yield.

R_f = 0.49 (5:1 (*v*/*v*) CH_2Cl_2/MeOH); ^{1}H NMR ($CDCl_3$, ppm): δ 4.17 (t, 2H, *J* = 1.7 Hz, Cp), 4.14 (s, 5H, Cp), 4.11 (t, 2H, *J* = 1.7 Hz, Cp), 3.55 (s, 2H, -C*H*$_2$ spacer); IR (NaCl plates, cm^{-1}): 3366, 3298, 3092, 2965, 2926, 2857, 1636, 1558, 1541, 1456, 1449, 1437, 1105, 1037, 1022, 1001, 817.

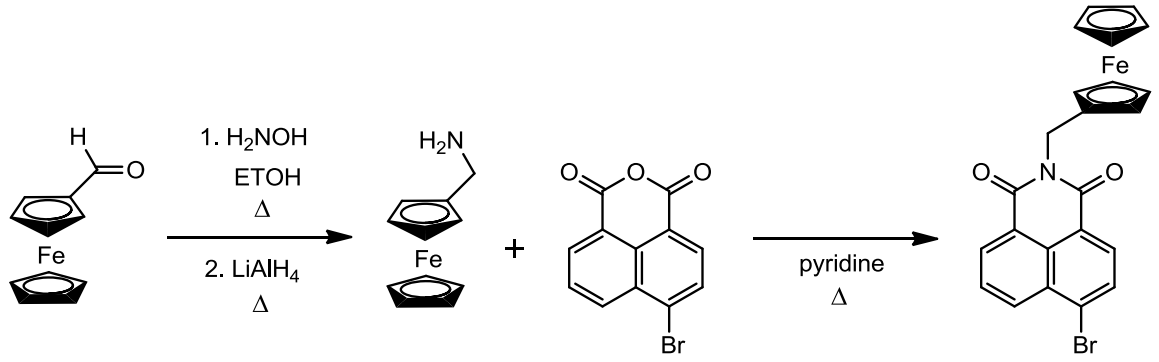

Scheme S1 Synthesis of ferrocenylmethylamine and *N*-ferrocenyl-4-bromo-1,8-naphthalimide.

Synthesis of *N*-ferrocenyl-4-bromo-1,8-naphthalimide

4-Bromo-1,8-naphthalic anhydride (0.440 g, 1.59 mmol) and ferrocenylmethylamine (0.371 g, 1.73 mmol) were dissolved in 25 mL of pyridine. The reaction mixture was stirred and refluxed at 125 °C for 18 hours under a nitrogen atmosphere. The reaction mixture was hydrolysed with 50 mL water and extracted with dichloromethane (3×25 mL). After drying with $MgSO_4$ and filtering the organic phase, the desired product was purified by column chromatography with silica gel and eluted with dichloromethane. The solvent was removed by rotatory evaporator. The product was collected as an orange solid in 64% yield.

R_f = 0.71 (CH_2Cl_2); m.p. = 230-233 °C (dec.); ^{1}H NMR ($CDCl_3$, ppm): δ 8.63 (dd, 1H, *J* = 7.4 Hz, 1.0, Ar-*H*), 8.53 (dd, 1H, *J* = 8.6, 1.0 Hz, Ar-*H*), 8.39 (d, 1H, *J* = 7.9 Hz, Ar-*H*), 8.00 (d, 1H, *J* = 7.9 Hz, Ar-*H*), 7.81 (dd, 1H, *J* = 7.9, 1.0 Hz, Ar-*H*), 5.12 (s, 2H, -C*H*$_2$ spacer), 4.50 (t, 2H, *J* = 1.8 Hz, Cp), 4.22 (s, 5H, Cp), 4.08 (t, 2H, *J* = 1.8 Hz, Cp); ^{13}C

NMR ($CDCl_3$, ppm): δ 163.3, 163.0, 133.2, 132.0, 131.2, 131.0, 130.5, 130.2, 128.9, 128.0, 123.2, 122.3, 82.8, 70.4, 68.7, 68.1, 39.4.

Synthesis of **1a**, *N*-ferrocenylmethyl-4-(2-dimethylaminoethylamine)-1,8-naphthalimide

N-ferrocenyl-4-bromo-1,8-naphthalimide (0.219 g, 0.462 mmol) and *N*,*N*-dimethylethylenediamine (5.0 mL, 46 mmol) were refluxed at 100 °C for 5 hours. The product was purified by column chromatography using silica gel and eluted with 4:1 (*v*/*v*) chloroform/methanol. Compound **1a** was collected as the second band. The recovered crude product was recrystallised from 1:1 (*v*/*v*) acetone/water to give an orange solid in 70% yield.

R_f = 0.73 (2:1 (*v*/*v*) CH_2Cl_2/MeOH); m.p. = 164-166 °C; ^{1}H NMR ($CDCl_3$, ppm): δ 8.55 (dd, 1H, *J* = 7.3, 0.9 Hz, Ar-*H*), 8.43 (d, 1H, *J* = 8.4 Hz, Ar-*H*), 8.10 (dd, 1H, *J* = 8.2, 0.9 Hz, Ar-*H*), 7.58 (dd, 1H, *J* = 7.8, 0.9 Hz, Ar-*H*), 6.63 (d, 1H, *J* = 8.5 Hz, Ar-*H*), 6.25 (m, 1H, -N*H*), 5.11 (s, 2H, -CH_2 spacer), 4.52 (t, 2H, *J* = 1.8 Hz, Cp), 4.20 (s, 5H, Cp), 4.06 (t, 2H, *J* = 1.8 Hz, Cp), 3.36 (m, 2H, -NHCH_2CH$_2$N), 2.72 (t, 2H, *J* = 5.8 Hz, -NHCH$_2$CH_2N), 2.33 (s, 6H, -N(CH_3)$_2$); ^{13}C NMR ($CDCl_3$, ppm): δ 164.5, 163.9, 149.6, 134.6, 131.1, 129.8, 126.4, 124.5, 123.1, 120.4, 110.1, 104.3, 83.8, 70.5, 68.6, 67.9, 56.9, 45.0, 40.1, 38.9; IR (KBr, cm^{-1}): 3393, 3092, 2955, 2866, 2828, 2783, 1684, 1636, 1582, 1541, 1385, 1369, 1339, 1300, 1246, 1188, 1126, 1105, 773; HRMS (ES-ToF): Calculated $C_{27}H_{28}N_3O_2Fe$ $[M+H]^+$ 482.1531, found 482.1521.

Synthesis of **1b**, *N*-ferrocenylmethyl-4-(2-aminoethylmorpholine)-1,8-naphthalimide

N-ferrocenyl-4-bromo-1,8-naphthalimide (0.759 g, 1.60 mmol) and 4-(2-aminoethyl)morpholino (0.50 mL, 11 mmol) were dissolved in 1,4-dioxane and refluxed for 4 hours at 95 °C. The reaction was quenched by adding 50 mL water and the crude product extracted with dichloromethane (3×30 mL). The organic phase was dried over anhydrous $MgSO_4$, filtered and the solvent removed by rotary evaporator. Purification was by column chromatography using silica gel eluted with dichloromethane followed by 50:1 (*v*/*v*) dichloromethane/methanol. The product was recrystallised from 1:1 (*v*/*v*) acetone/water to give an orange solid in 13% yield.

R_f = 0.53 (20:1 (*v*/*v*) CH_2Cl_2/MeOH); m.p. = 218-224 °C (dec.); ^{1}H NMR ($CDCl_3$, ppm): δ 8.56 (dd, 1H, *J* = 7.3, 0.9 Hz, Ar-*H*), 8.43 (d, 1H, *J* = 8.4 Hz, Ar-*H*), 8.04 (dd, 1H, *J* = 8.5, 0.9 Hz, Ar-*H*), 7.60 (dd, 1H, *J* = 7.9, 0.9 Hz, Ar-*H*), 6.63 (d, 1H, *J* = 8.5 Hz, Ar-*H*), 6.21 (m, 1H, -N*H*), 5.11 (s, 2H, -CH_2 spacer), 4.52 (t, 2H, *J* = 1.8 Hz, Cp), 4.20 (s, 5H, Cp), 4.06 (t, 2H, *J* = 1.8 Hz, Cp), 3.78 (t, 4H, *J* = 4.5 Hz, -N(CH_2CH_2)$_2$O), 3.41 (m, 2H, -NHCH_2CH_2N), 2.82 (t, 2H, *J* = 5.9 Hz, -NHCH_2CH_2N), 2.57 (m, 4H, -N(CH_2CH_2)$_2$O); ^{13}C NMR ($CDCl_3$, ppm): δ 164.4, 163.8, 149.3, 134.4, 131.1, 129.6, 125.9, 124.7, 123.2, 120.3, 110.3, 104.4, 83.7, 70.5, 68.6, 67.9, 67.1, 56.0, 53.1, 38.9 (two peaks); IR (KBr, cm^{-1}): 3416, 3362, 3084, 2963, 2818, 1684, 1647, 1582, 1533, 1368, 1344, 1333, 1300, 1246, 1188, 1134, 1117, 1103, 775; HRMS (ES-ToF): Calculated $C_{29}H_{30}N_3O_3Fe$ $[M+H]^+$ 524.1637, found 524.1639.

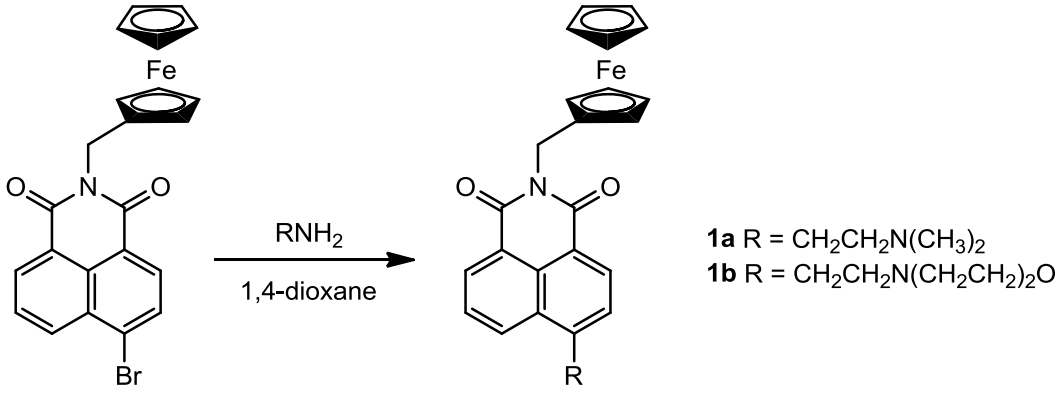

Scheme S2: Synthesis of compounds **1a** and **1b**.

Synthesis of *N*,*N*-dimethylethylenediamine-4-bromo-1,8-naphthalimide

4-Bromo-1,8-naphthalic anhydride (2.59 g, 9.33 mmol) was dissolved in 25 mL of 1,4-dioxane and *N*,*N*-dimethylethylenediamine (0.807 g/ 1.00 mL, 9.15 mmol) was added and refluxed at 95 °C for 3 hours. The reaction mixture was hydrolysed with 50 mL water and extracted with dichloromethane (3×25 mL). The solution was dried over $MgSO_4$, filtered and purified by recrystallisation from 4:4:1 (*v*/*v*/*v*) dichloromethane/diethyl ether/hexane. Intermediate **6** was collected as an off-white solid in 70% yield.

R_f = 0.52 (20:1 (*v*/*v*) CH_2Cl_2/MeOH); m.p. = 152-153 °C; ^{1}H NMR ($CDCl_3$, ppm): δ 8.65 (dd, 1H, *J* = 7.3, 1.1 Hz, Ar-*H*), 8.57 (dd, 1H, *J* = 8.5, 1.1 Hz, Ar-*H*), 8.41 (d, 1H, *J* = 7.9 Hz, Ar-*H*), 8.04 (d, 1H, *J* = 7.9 Hz, Ar-*H*), 7.84 (dd, 1H, *J* = 7.9, 1.1 Hz, Ar-*H*), 4.32 (t, 2H, *J* = 7.0 Hz, -NC*H*$_2$CH$_2$N(CH$_3$)$_2$), 2.65 (t, 2H, *J* = 7.0 Hz, -NCH$_2$C*H*$_2$N(CH$_3$)$_2$), 2.35 (s, 6H, -N(C*H*$_3$)$_2$); ^{13}C NMR ($CDCl_3$, ppm): δ 163.64, 163.62, 133.2, 132.1, 131.2, 131.1, 130.6, 130.2, 129.0, 128.1, 123.1, 122.2, 57.0, 45.8, 38.3; HRMS (ES-ToF): Calculated $C_{16}H_{16}N_2O_2Br$ $[M+H]^+$ 347.0395, found 347.0411.

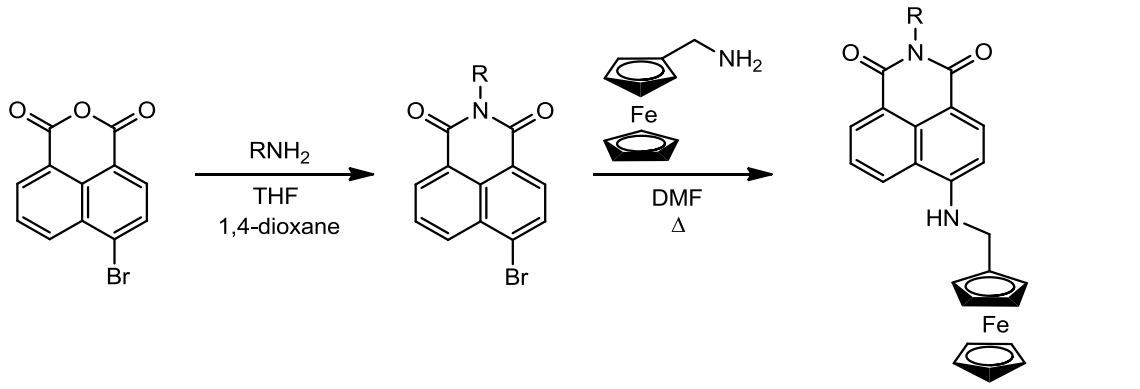

2a R = $CH_2CH_2N(CH_3)_2$
2b R = $CH_2CH_2N(CH_2CH_2)_2O$

Scheme S3: Synthesis of compounds **2a** and **2b**.

Synthesis of 4-(2-aminoethyl)morpholine-4-bromo-1,8-naphthalimide

4-Bromo-1,8-naphthalic anhydride (0.997 g, 3.60 mmol) and 4-(2-aminoethyl)morpholine (0.496 g/ 0.50 mL, 3.81 mmol) were dissolved in 25 mL of 1,4-dioxane. The reaction mixture was stirred and refluxed at 95 °C for 1 hour. The reaction mixture was hydrolysed with 50 mL water and extracted with dichloromethane (3×30 mL), dried over anhydrous $MgSO_4$, filtered and purified by column chromatography eluting with 96:4 (*v*/*v*) dichloromethane/methanol to give an off-white solid in 46% yield. R_f = 0.57 (20:1 (*v*/*v*) CH_2Cl_2/MeOH); m.p. = 168-170 °C; ^{1}H NMR ($CDCl_3$, ppm): δ 8.65 (dd, 1H, *J* = 7.3, 1.1 Hz, Ar-*H*), 8.57 (dd, 1H, *J* = 8.5, 1.1 Hz, Ar-*H*), 8.41 (d, 1H, *J* = 7.9 Hz, Ar-*H*), 8.04 (d, 1H, *J* = 7.9 Hz, Ar-*H*), 7.85 (dd, 1H, *J* = 7.9, 1.1 Hz, Ar-*H*), 4.33 (t, 2H, *J* = 6.9 Hz, -NC*H*$_2$CH$_2$N(CH$_2$CH$_2$)$_2$O), 3.67 (t, 4H, *J* = 4.6 Hz, -NCH$_2$CH$_2$N(CH$_2$C*H*$_2$)$_2$O), 2.70 (t, 2H, *J* = 6.9 Hz, -NCH$_2$C*H*$_2$N(CH$_2$CH$_2$)$_2$O), 2.59 (m, 4H, -NCH$_2$CH$_2$N(C*H*$_2$CH$_2$)$_2$O); ^{13}C NMR ($CDCl_3$, ppm): δ 163.62, 163.60, 133.3, 132.0,

131.2, 131.1, 130.7, 130.3, 129.0, 128.1, 123.1, 122.2, 67.1, 56.1, 53.8, 37.4; HRMS (ES-ToF): Calculated $C_{18}H_{18}N_2O_3Br$ $[M+H]^+$ 389.0501, found 389.0520.

Synthesis of **2a**, *N*,*N*-dimethylethylenediamine-4-*N*-ferrocenylmethyl-1,8-naphthalimide

N,*N*-dimethylethylenediamine-4-bromo-1,8-naphthalimide (0.440 g, 1.27 mmol) and ferrocenylmethylamine (0.301 g, 1.40 mmol) were dissolved in 10 mL of DMF. The reaction mixture was stirred and refluxed at 75 °C for 72 hours. The reaction mixture was hydrolysed with 25 mL water and **8** was extracted with diethyl ether (4×20 mL). Anhydrous $MgSO_4$ was used to dry the organic phase, then filtered and purified via column chromatography loaded with silica gel eluted with diethyl ether followed by 20:1 (*v*/*v*) diethyl ether/methanol, 5:1 (*v*/*v*) diethyl ether/methanol, 1:1 (*v*/*v*) diethyl ether/methanol and 5:1 (*v*/*v*) methanol/acetone. The product **2a** was obtained as a reddish orange solid in 34% yield.

R_f = 0.51 (3:1 (*v*/*v*) $(CH_3CH_2)_2O$/MeOH); m.p. = 165-170 °C (dec.); ^{1}H NMR ($CDCl_3$, ppm): δ 8.60 (dd, 1H, *J* = 7.4, 0.9 Hz, Ar-*H*), 8.50 (d, 1H, *J* = 8.4 Hz, Ar-*H*), 8.07 (dd, 1H, *J* = 8.5, 0.9 Hz, Ar-*H*), 7.64 (t, 1H, *J* = 7.9, 0.9 Hz, Ar-*H*), 6.80 (d, 1H, *J* = 8.4 Hz, Ar-*H*), 5.46 (t, 1H, *J* = 4.5 Hz, -N*H*), 4.35 (t, 2H, *J* = 1.8 Hz, Cp), 4.33 (t, 2H, *J* = 7.2 Hz, -NC*H*$_2$CH$_2$N(CH$_3$)$_2$), 4.25-4.28 (m, 7H, Cp), 4.23 (d, 2H, *J* = 4.5 Hz, -HC*H*$_2$Cp), 2.66 (t, 2H, *J* = 7.2 Hz, -NCH$_2$C*H*$_2$N(CH$_3$)$_2$), 2.37 (s, 6H, -NCH$_2$CH$_2$N(C*H*$_3$)$_2$); ^{13}C NMR ($CDCl_3$, ppm): δ164.7, 164.2, 148.8, 134.6, 131.2, 130.9, 125.7, 124.9, 123.2, 120.1, 110.6, 104.5, 84.2, 68.7, 68.6, 68.4, 57.1, 45.7, 43.1, 37.9; IR (KBr, cm^{-1}): 3441, 3084, 2944, 2860, 2820, 2773, 1734, 1684, 1653, 1648, 1636, 1577, 1541, 1506, 1456, 1362, 1339, 1242, 1124, 775; HRMS (ES-ToF): Calculated $C_{27}H_{28}N_3O_2Fe$ $[M+H]^+$ 482.1531, found 482.1530.

Synthesis of **2b**, 4-(2-aminoethyl)morpholine-4-*N*-ferrocenylmethyl-1,8-naphthalimide

4-(2-aminoethyl)morpholine-4-bromo-1,8-naphthalimide (0.375 g, 0.960 mmol) and ferrocenylmethylamine (0.315 g, 1.47 mmol) were dissolved in 10 mL DMF. The reaction mixture was stirred and refluxed at 90 °C for 5 hours and then hydrolysed with 25 mL water and **2b** was extracted with dichloromethane (3×25 mL). Anhydrous $MgSO_4$

was used to dry the organic phase, filtered and the product purified via column chromatography loaded with silica gel and eluted with diethyl ether followed by 20:1 (*v*/*v*) diethyl ether/methanol, 10:1 (*v*/*v*) diethyl ether/methanol and 100:15 (*v*/*v*) diethyl ether/methanol. The solvent was removed by rotary evaporator to give a reddish orange solid in 22% yield.

R_f = 0.40 ($(CH_3CH_2)_2O$); m.p. = 94-98 °C; ^{1}H NMR ($CDCl_3$, ppm): δ 8.57 (dd, 1H, *J* = 7.3, 1.1 Hz, Ar-*H*), 8.47 (d, 1H, *J* = 8.2 Hz, Ar-*H*), 8.44 (dd, 1H, *J* = 8.5, 1.1 Hz, Ar-*H*), 7.66 (dd, 1H, *J* = 7.9, 1.1 Hz, Ar-*H*), 7.12 (d, 1H, *J* = 8.2 Hz, Ar-*H*), 5.70 (m, 1H, -N*H*), 4.33 (t, 2H, *J* = 7.1 Hz, -NC*H*$_2$CH$_2$N(CH$_2$CH$_2$)$_2$O), 4.20 (d, 2H, *J* = 5.6 Hz, -NHC*H*$_2$Cp), 4.19 (t, 2H, *J* = 1.8 Hz, Cp), 4.17 (s, 5H, Cp), 4.15 (t, 2H, *J* = 1.8 Hz, Cp), 3.69 (t, 4H, *J* = 4.6 Hz, -NCH$_2$CH$_2$N(CH$_2$C*H*$_2$)$_2$O), 2.70 (t, 2H, *J* = 7.1 Hz, -NCH$_2$C*H*$_2$N(CH$_2$CH$_2$)$_2$O), 2.59 (m, 4H, -NCH$_2$CH$_2$N(C*H*$_2$CH$_2$)$_2$O); ^{13}C NMR ($CDCl_3$, ppm): δ 164.6, 164.1, 160.1, 132.7, 131.2, 131.0, 125.3, 124.9, 123.1, 115.0, 113.4, 84.1, 68.6, 68.3, 68.2, 67.1, 56.2, 53.8, 44.8, 37.5; IR (KBr, cm^{-1}): 3320, 3080, 2953, 1684, 1657, 1655, 1589, 1456, 1423, 1390, 1381, 1346, 1242, 1142, 1113, 1009, 864, 779; HRMS (ES-ToF): Calculated $C_{29}H_{30}N_3O_3Fe$ $[M+H]^+$ 524.1637, found 524.1633.

References

S1. A. D. Johnson, K. A. Paterson, J. C. Spiteri, S. A. Denisov, G. Jonusauskas, A. Tron, N. D. McClenaghan and D. C. Magri, *New J. Chem.*, 2016, 40, 9917.

S2. P. D. Beer and D. K. Smith, *J. Chem. Soc., Dalton Trans*., 1998, 417.

S3. A. Baramee, A. Coppin, M. Mortuaire, L. Pelinski, S. Tomavo and J. Brocard, *Bioorg. Med. Chem*., 2006, **14**, 1294.

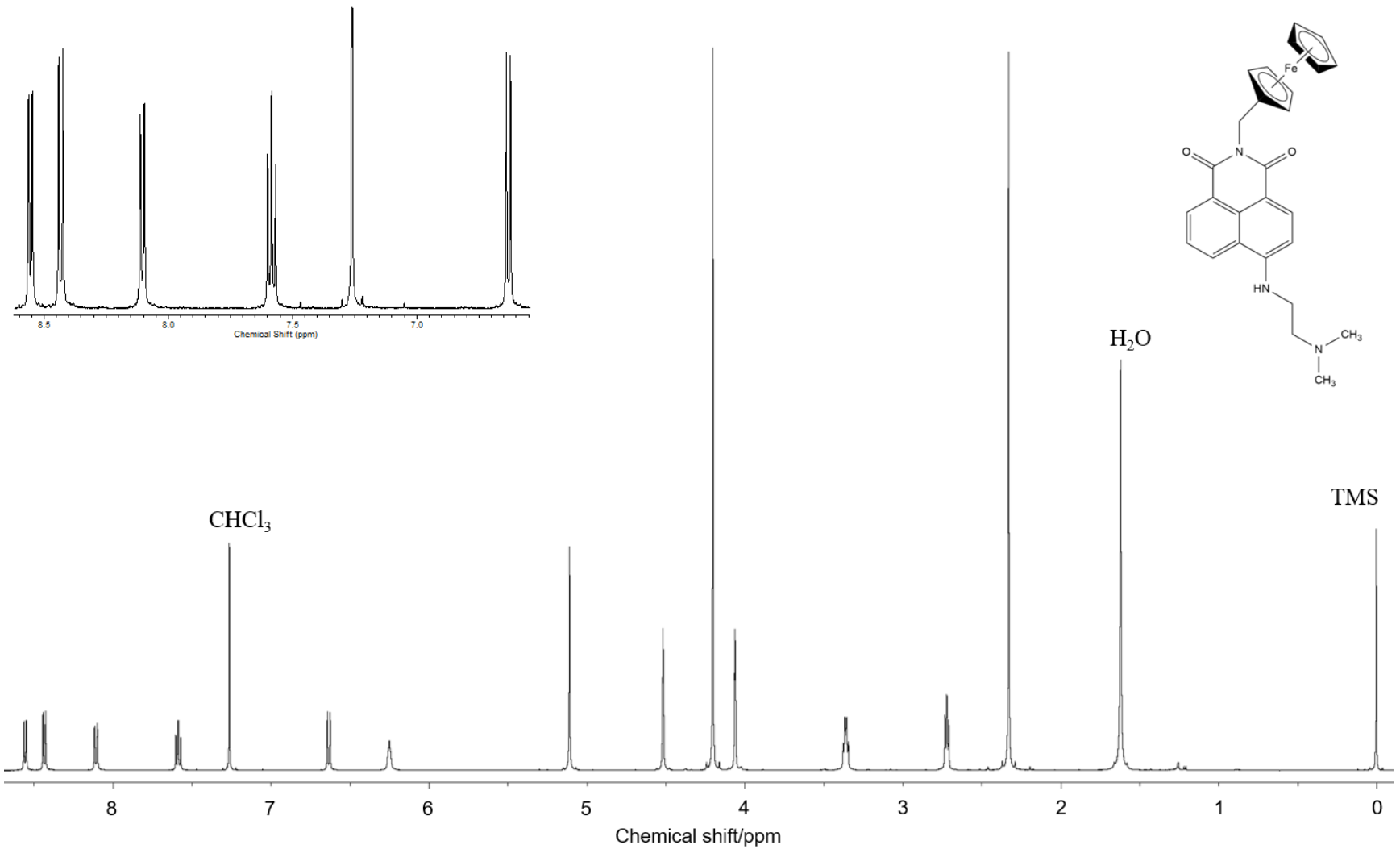

Fig. S1 ^{1}H NMR spectrum of **1a** in $CDCl_3$ at 500 MHz.

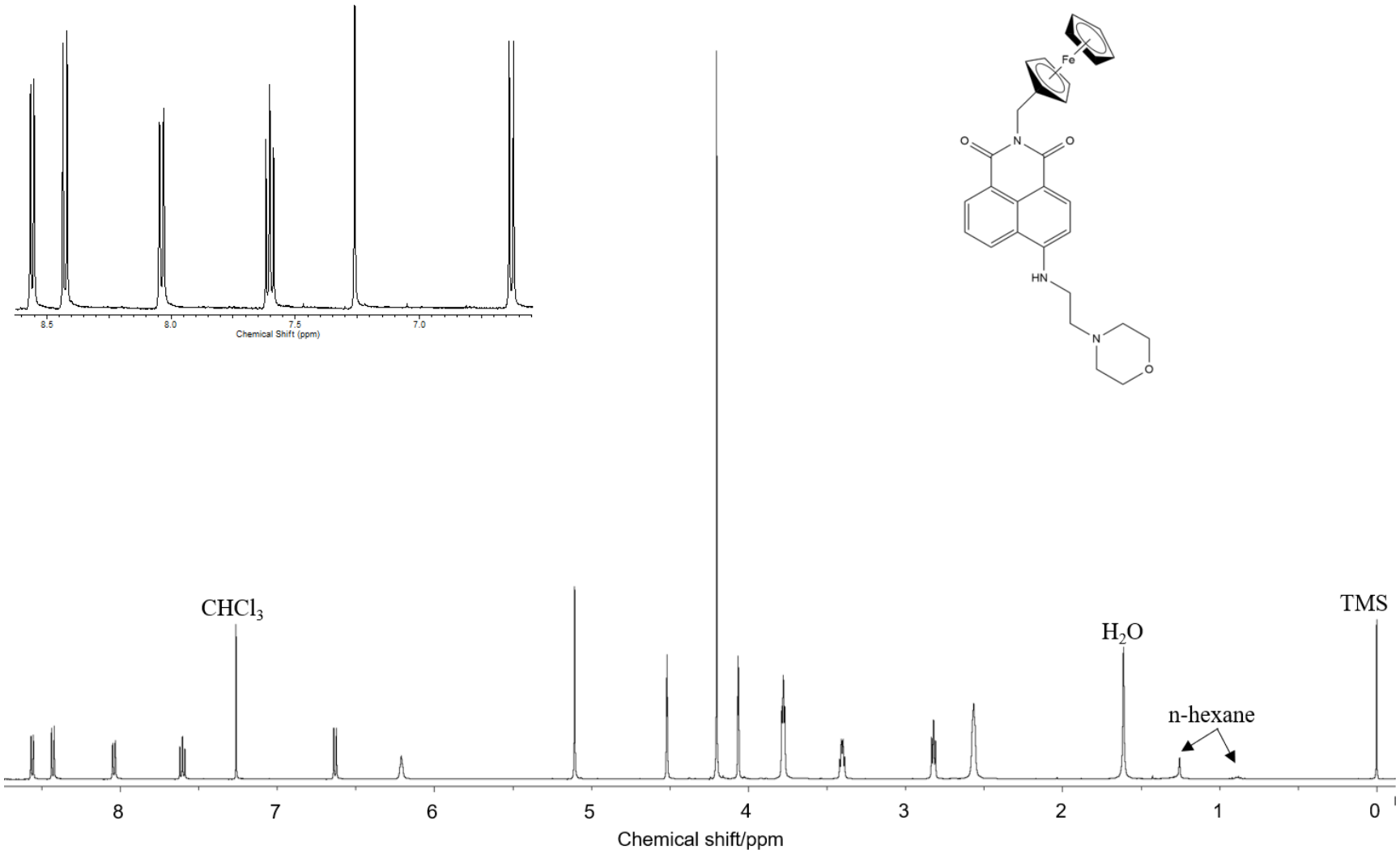

Fig. S2 ^{1}H NMR spectrum of **1b** in $CDCl_3$ at 500 MHz.

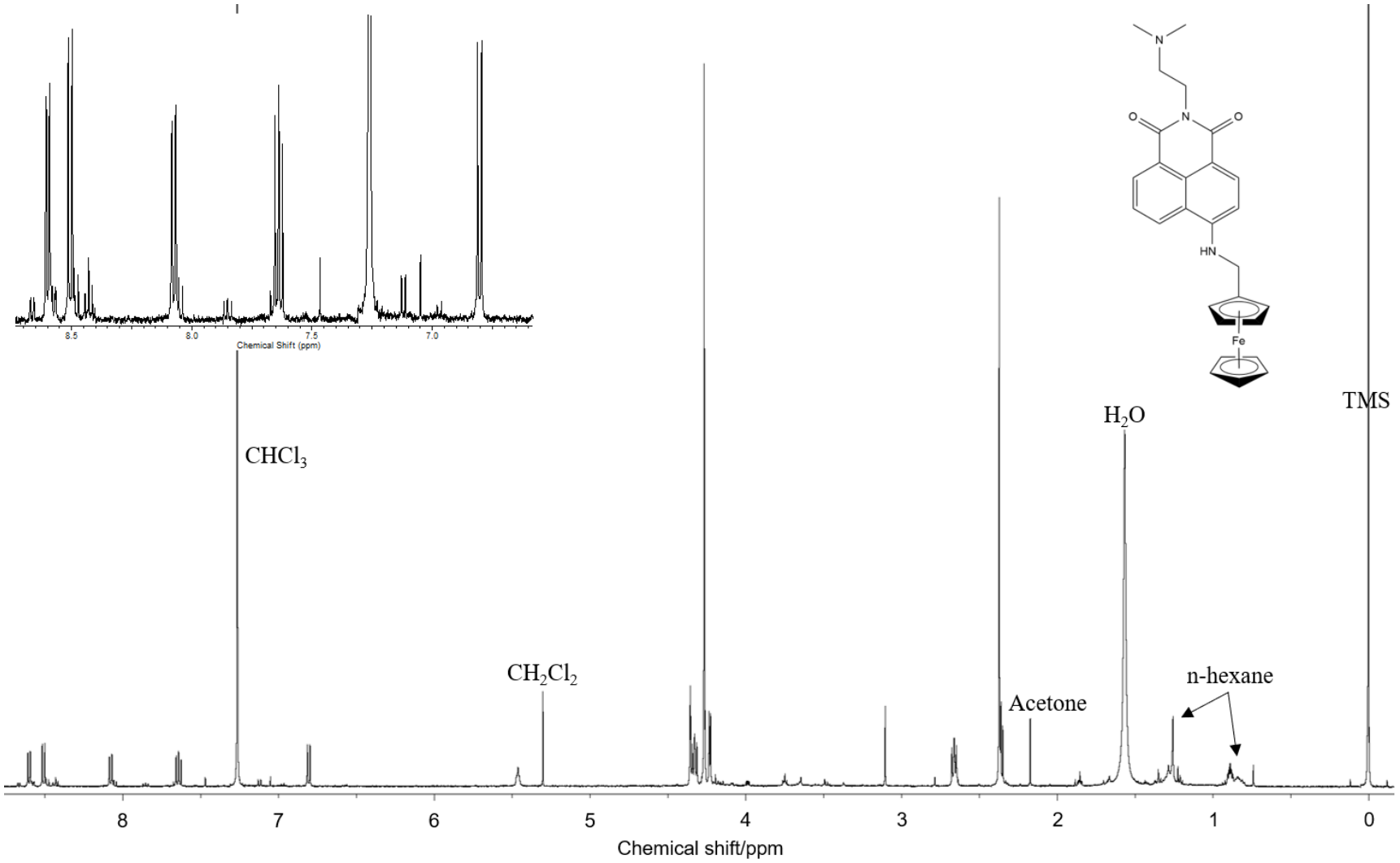

Fig. S3 ^{1}H NMR spectrum of **2a** in $CDCl_3$ at 500 MHz.

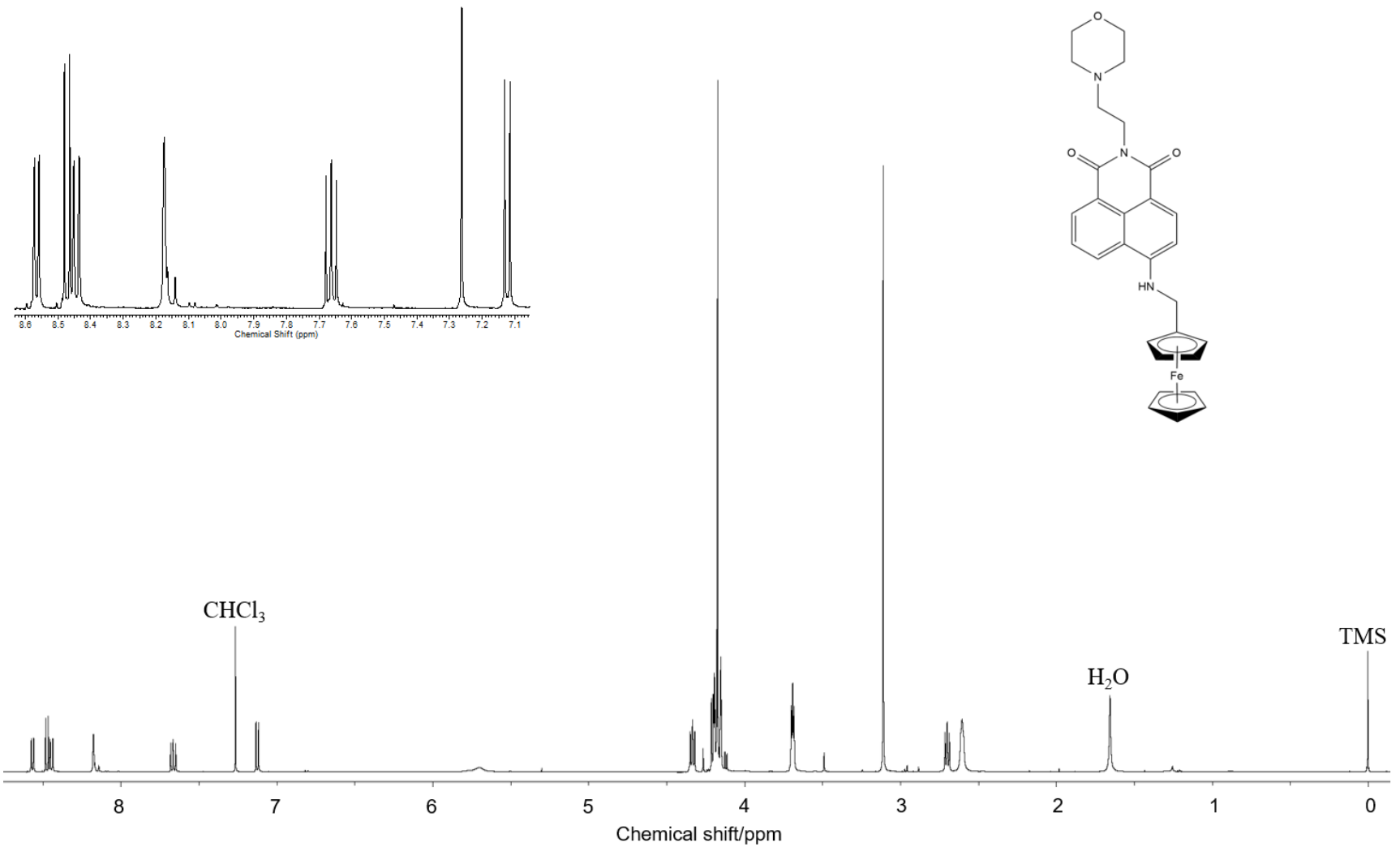

Fig. S4 ^{1}H NMR spectrum of **2b** in $CDCl_3$ at 500 MHz.

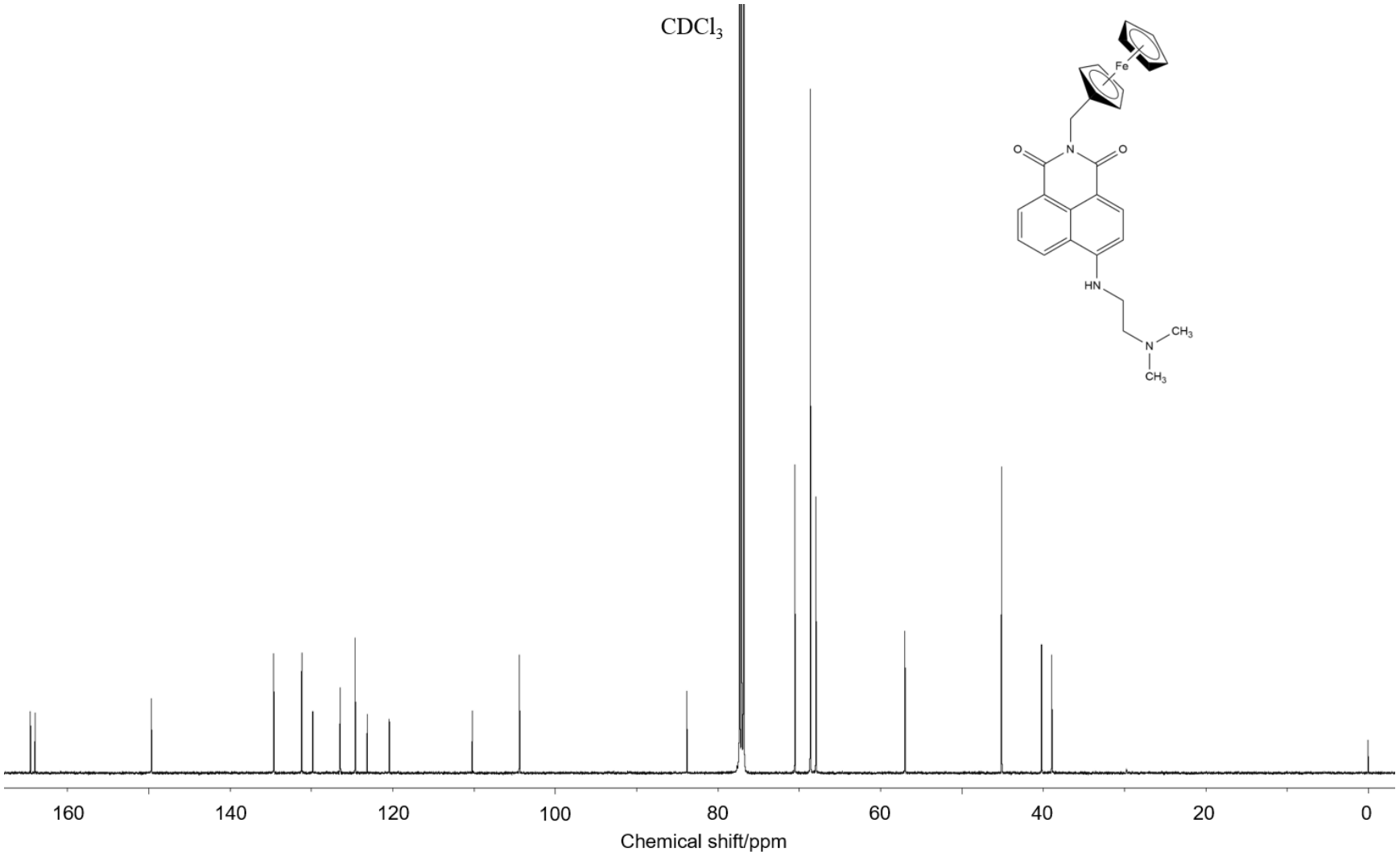

Fig. S5 ^{13}C NMR spectrum of **1a** in $CDCl_3$ at 126 MHz.

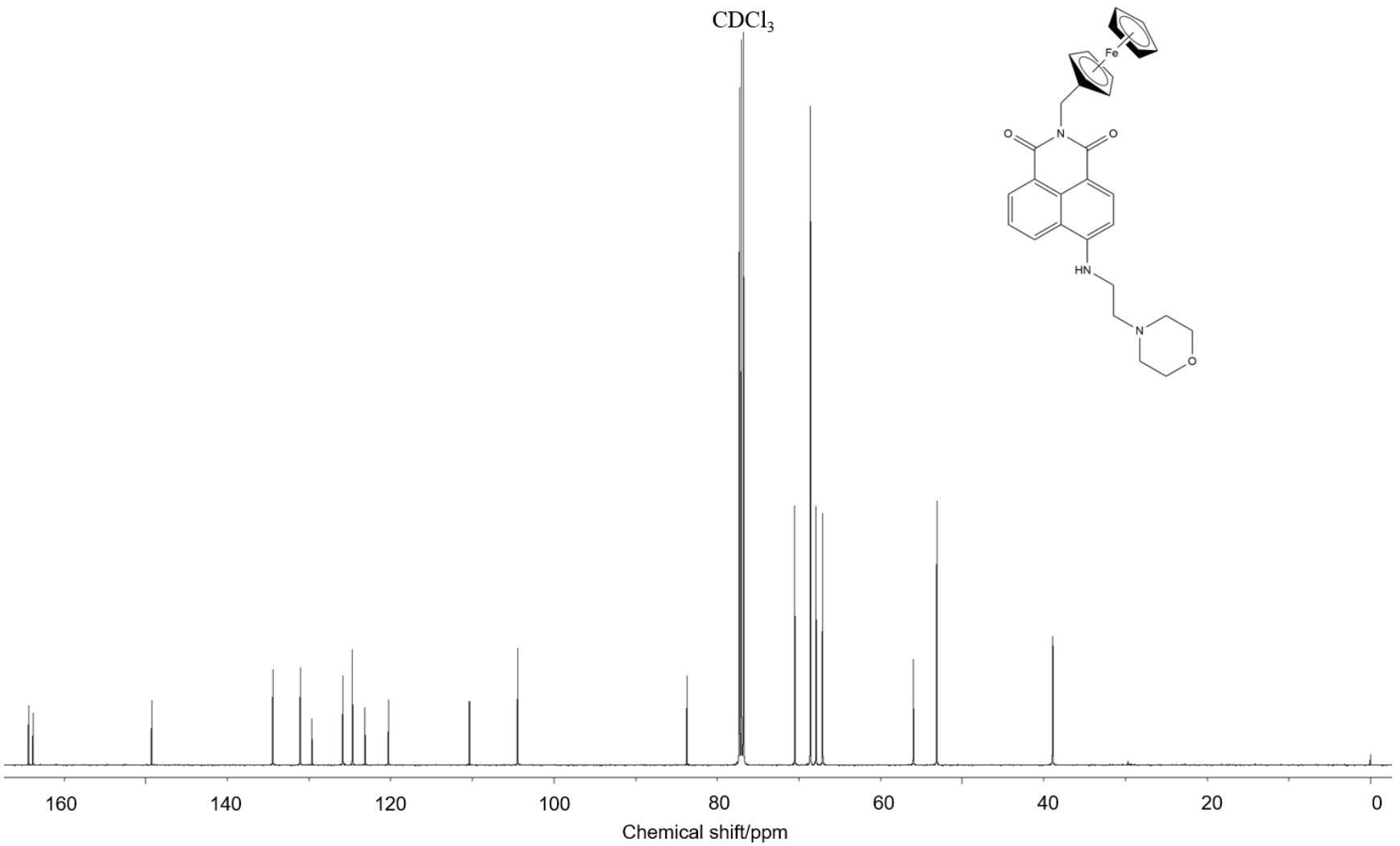

Fig. S6 ^{13}C NMR spectrum of **1b** in $CDCl_3$ at 126 MHz.

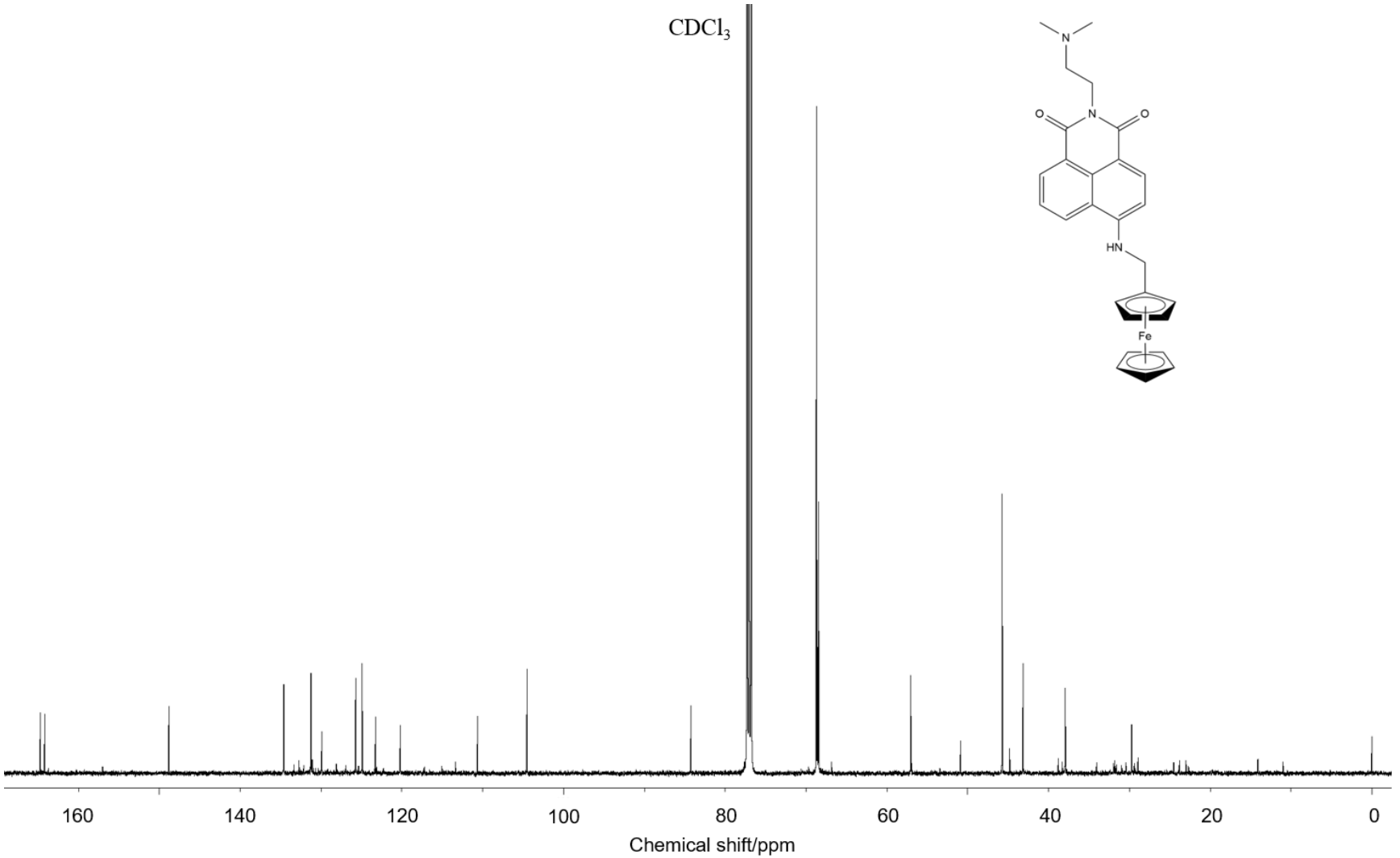

Fig. S7 ^{13}C NMR spectrum of **2a** in $CDCl_3$ at 126 MHz.

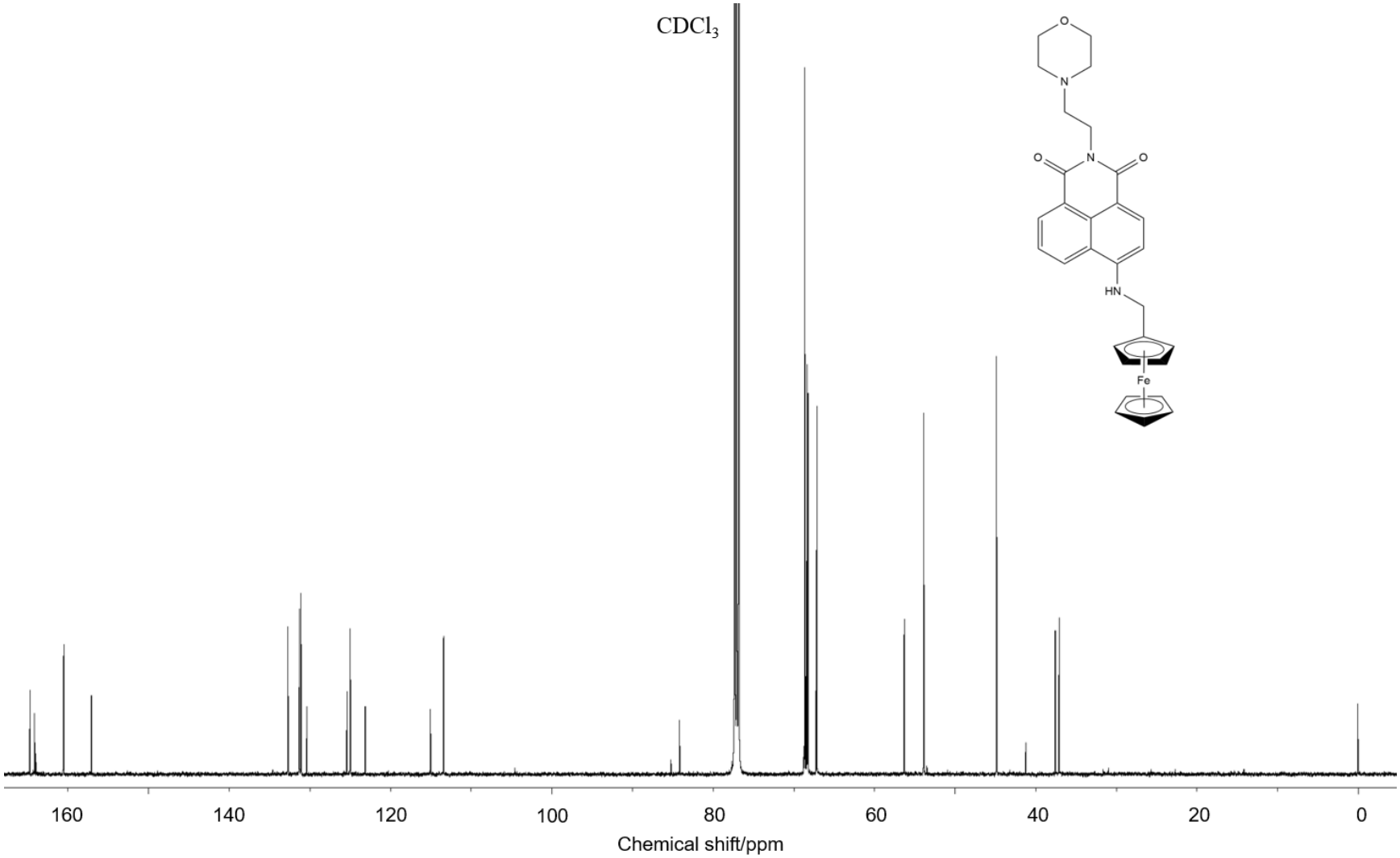

Fig. S8 ^{13}C NMR spectrum of **2b** in $CDCl_3$ at 126 MHz.

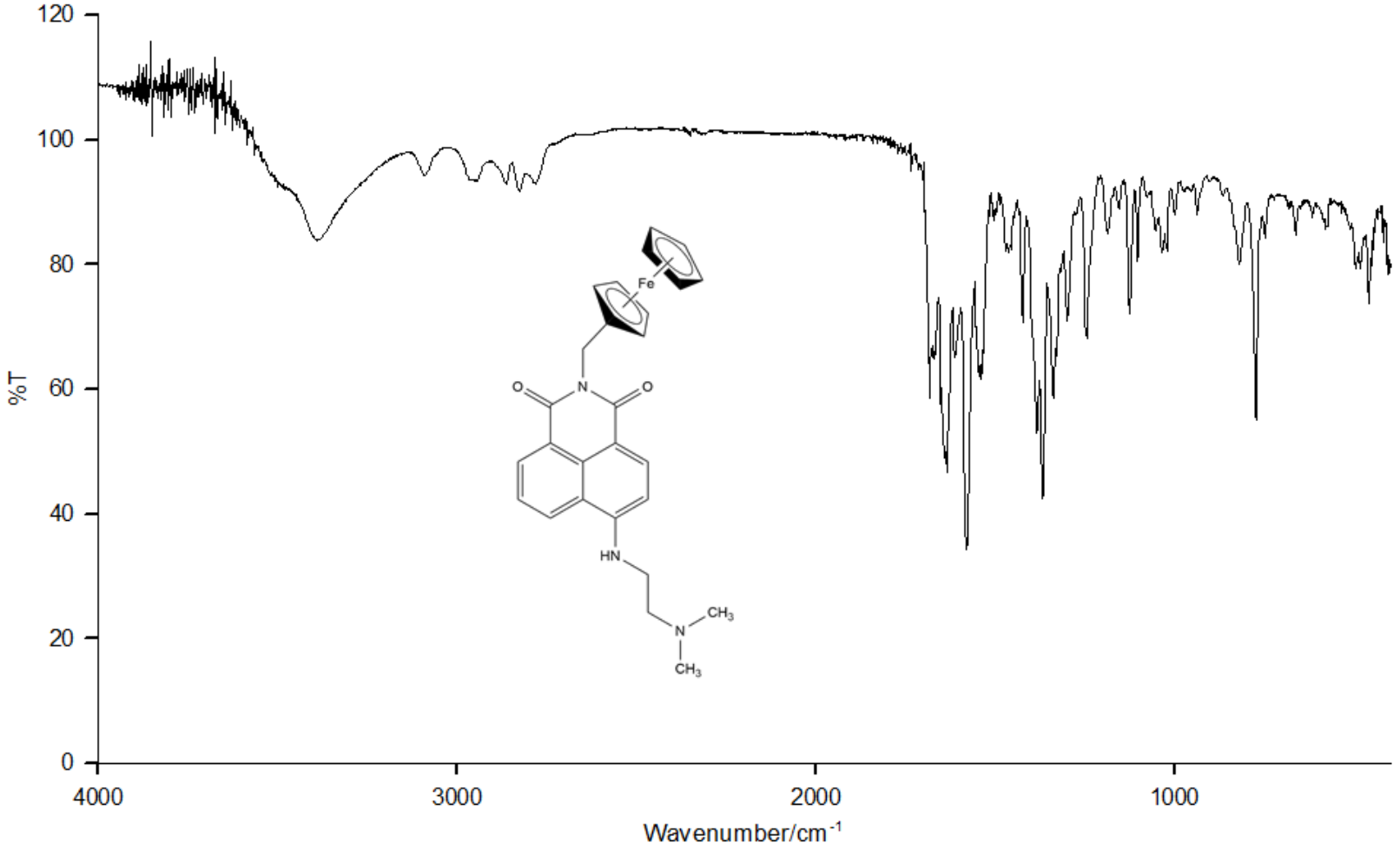

Fig. S9 IR spectrum of **1a** (KBr disk).

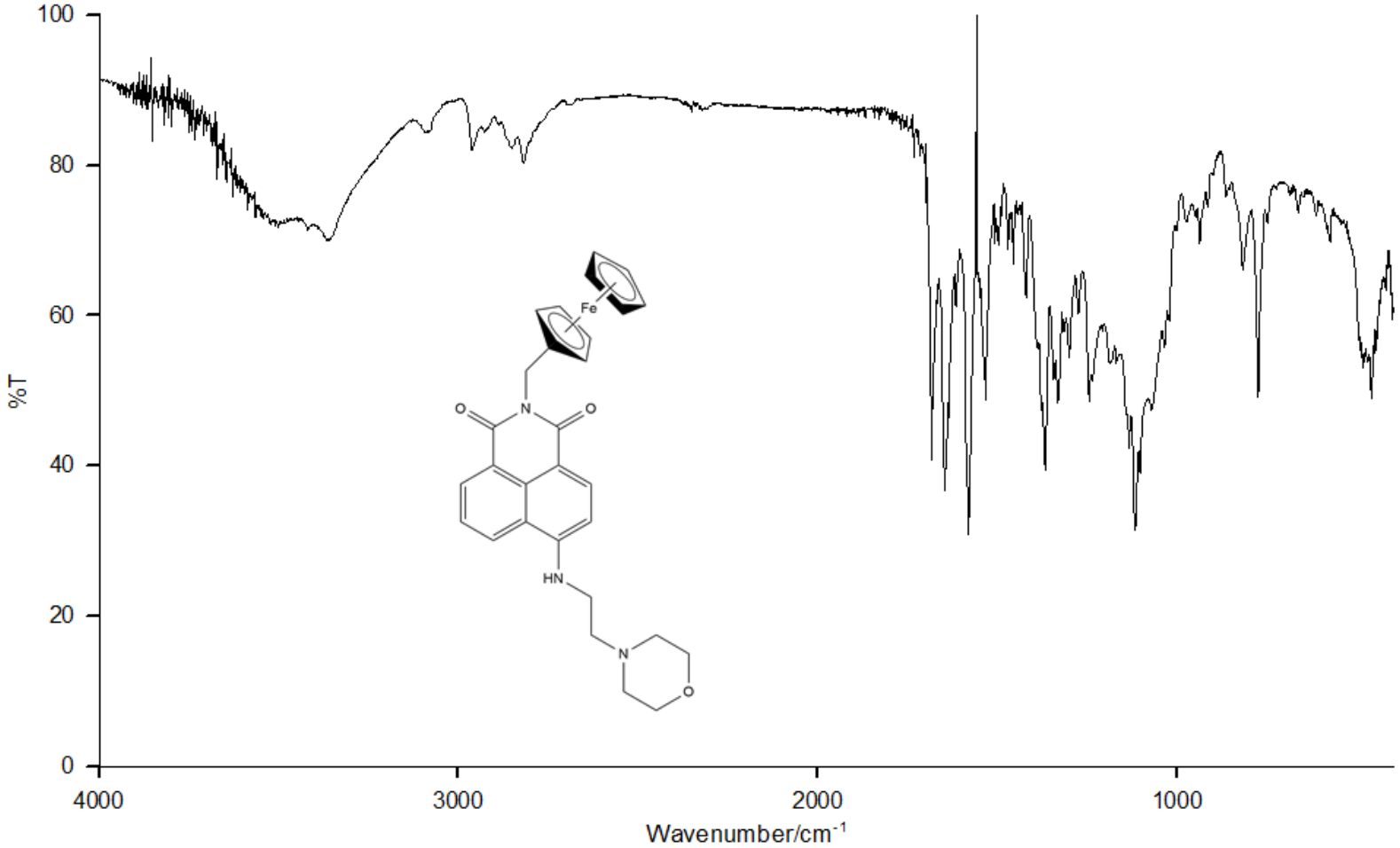

Fig. S10 IR spectrum of **1b** (KBr disk).

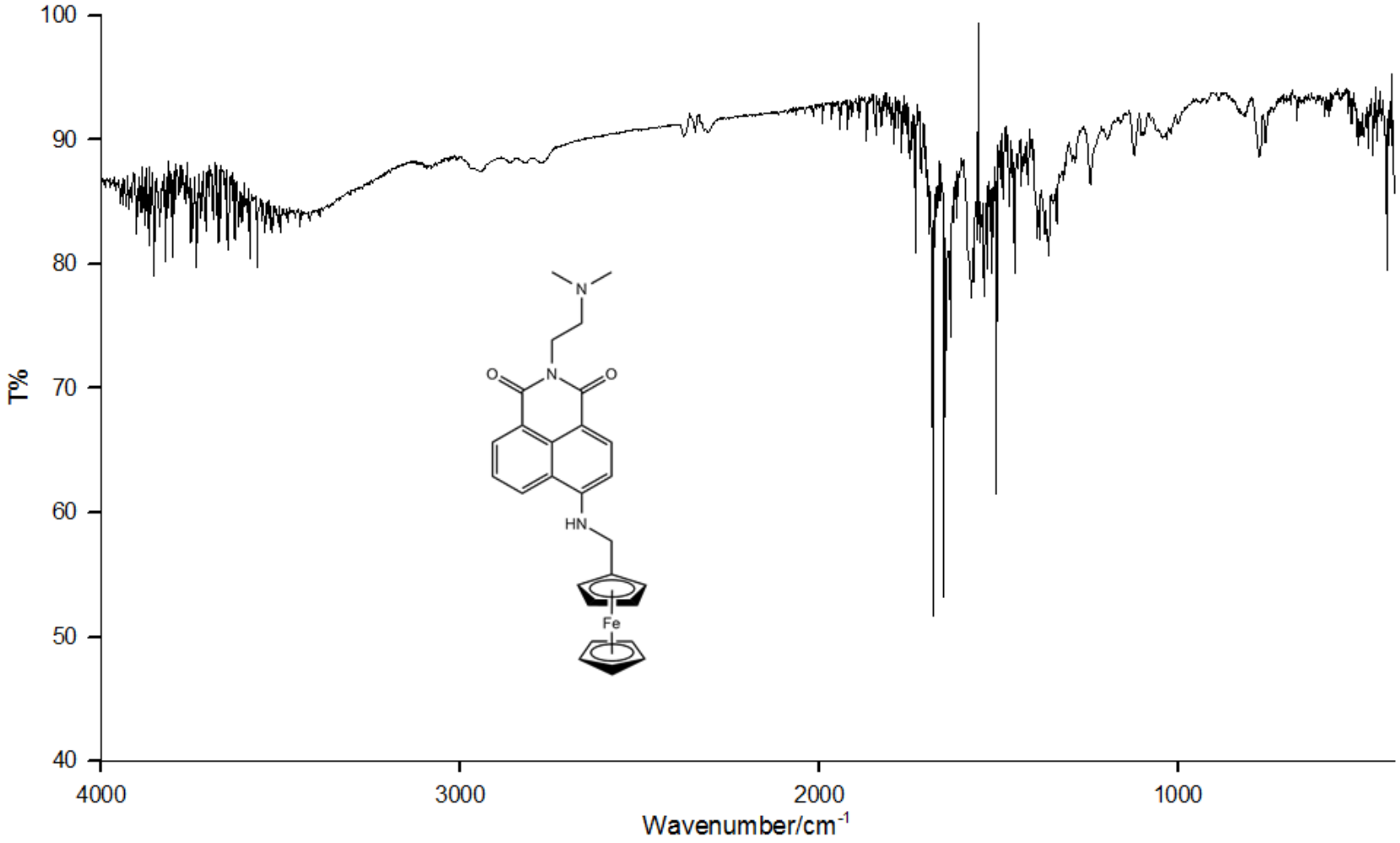

Fig. S11 IR spectrum of **2a** (KBr disk).

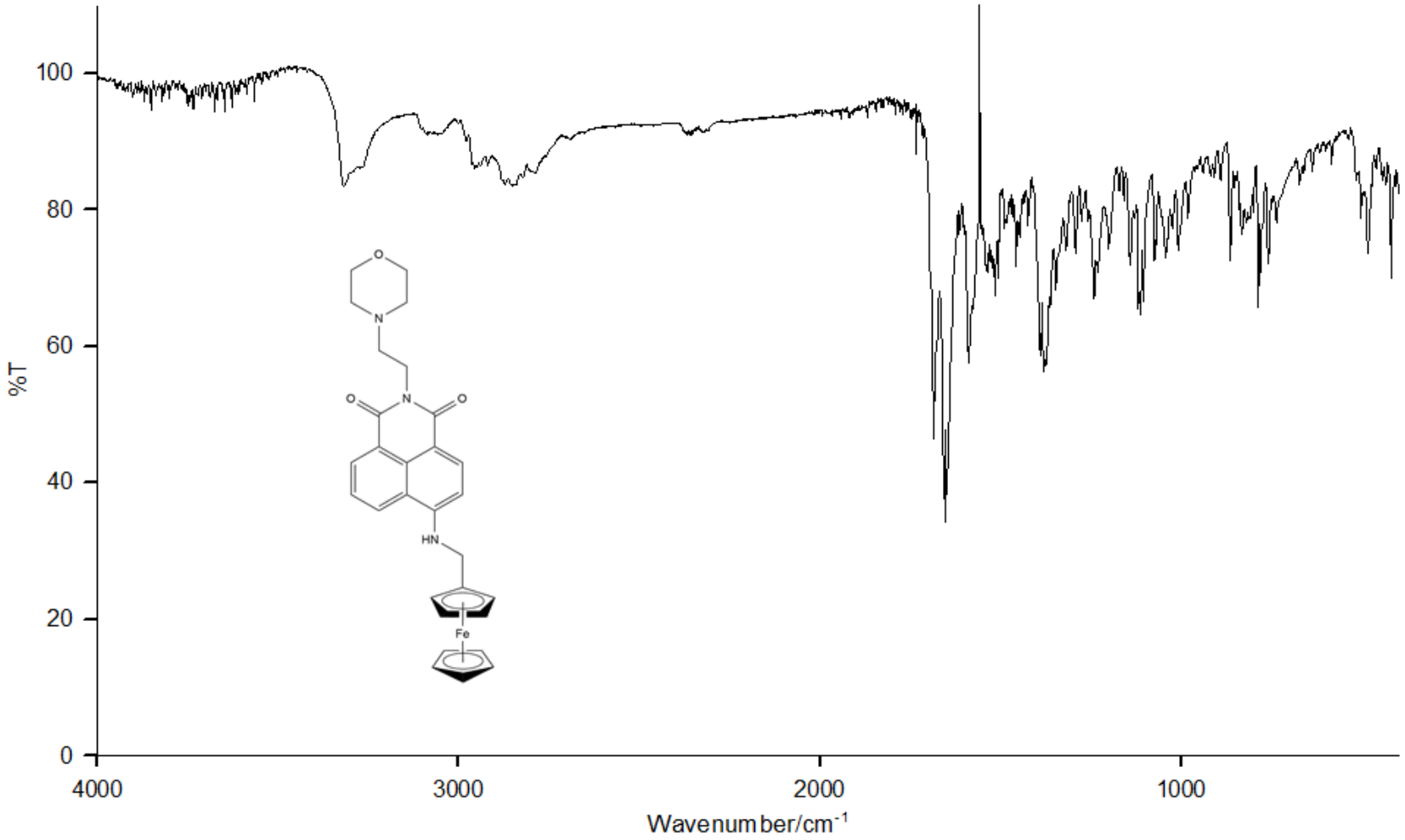

Fig. S12 IR spectrum of **2b** (KBr disk).

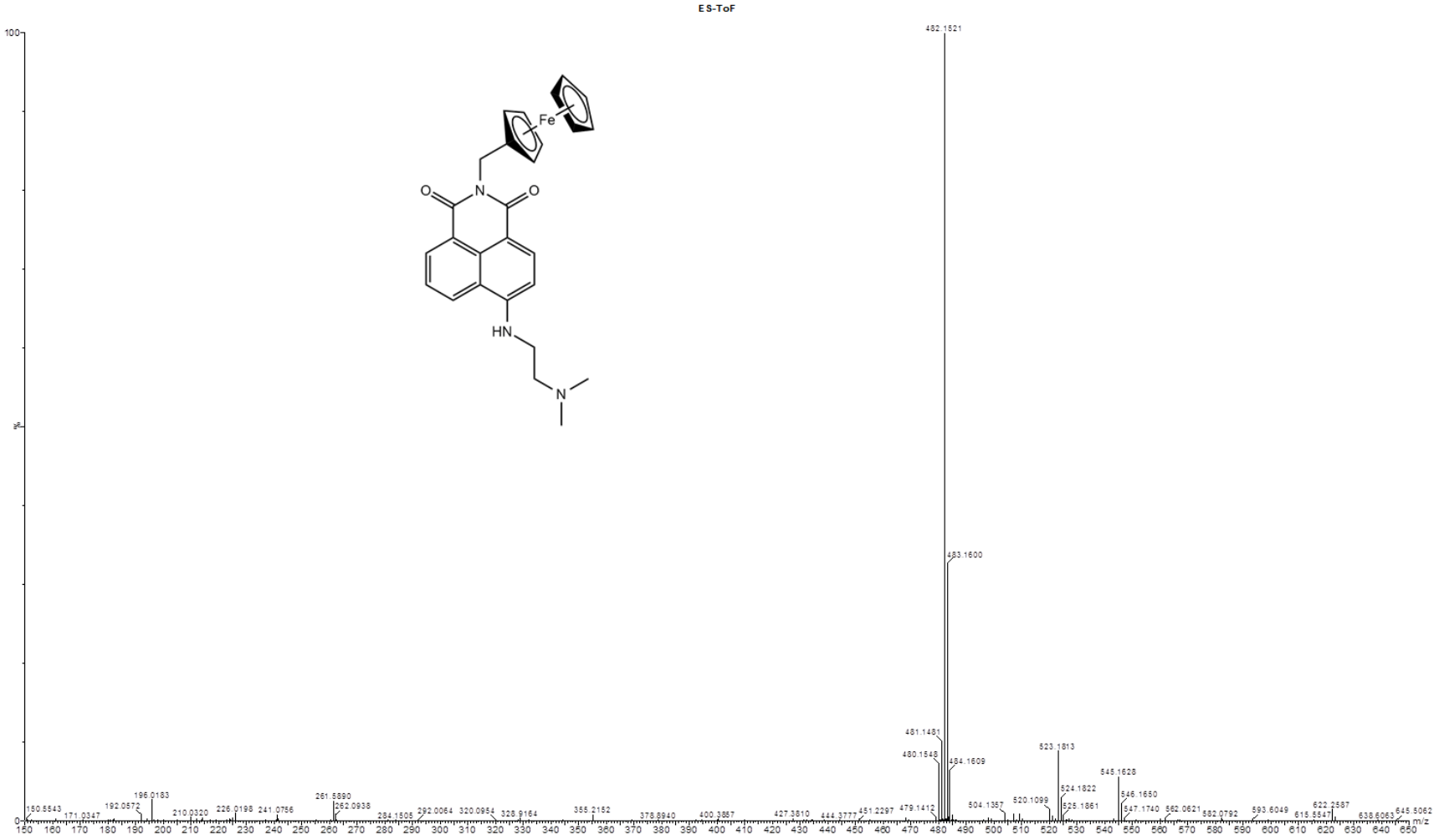

Fig. S13 High resolution MS of **1a** by electrospray time-of-flight mass technique.

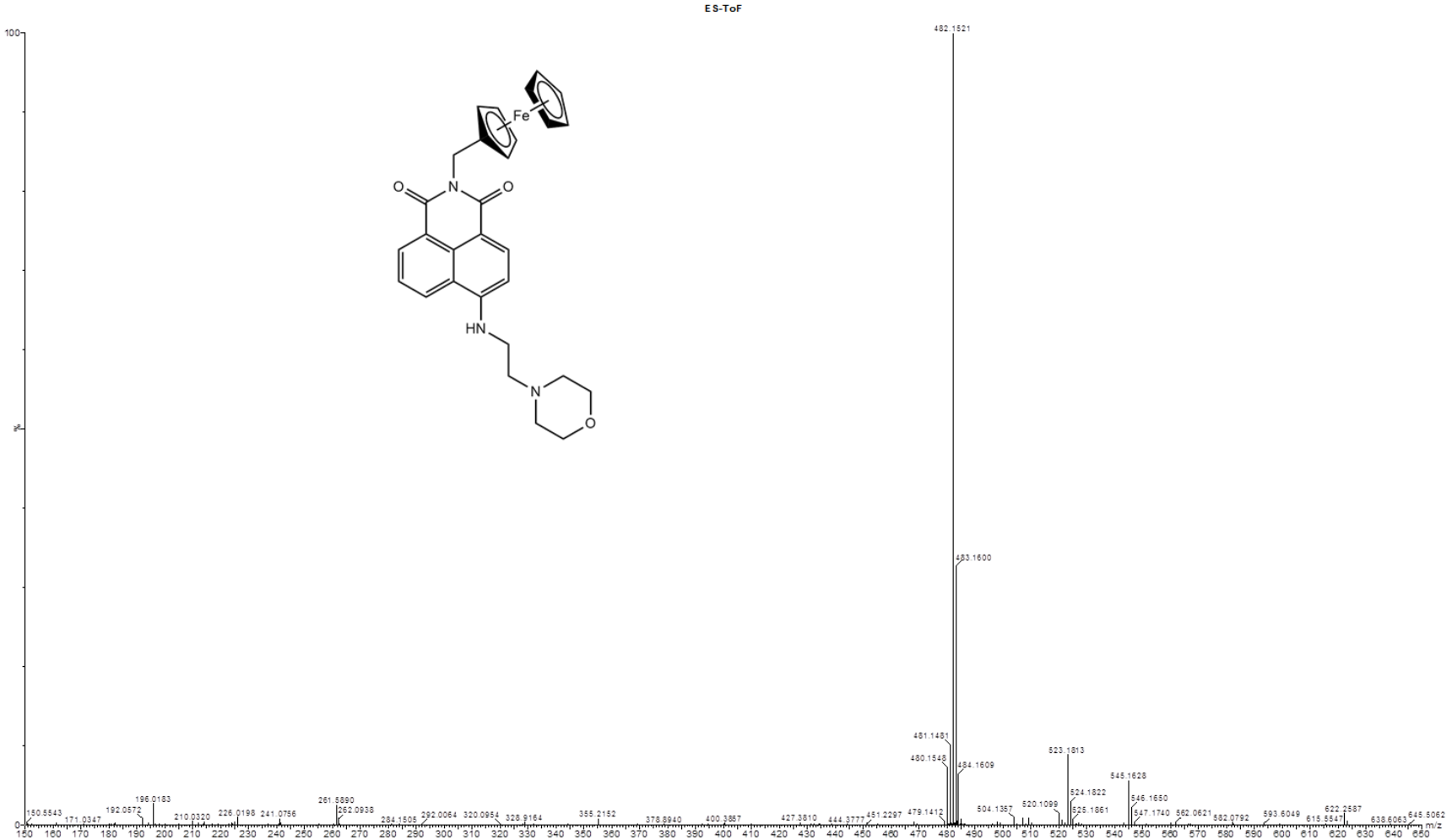

Fig. S14 High resolution MS of **1b** by electrospray time-of-flight mass technique.

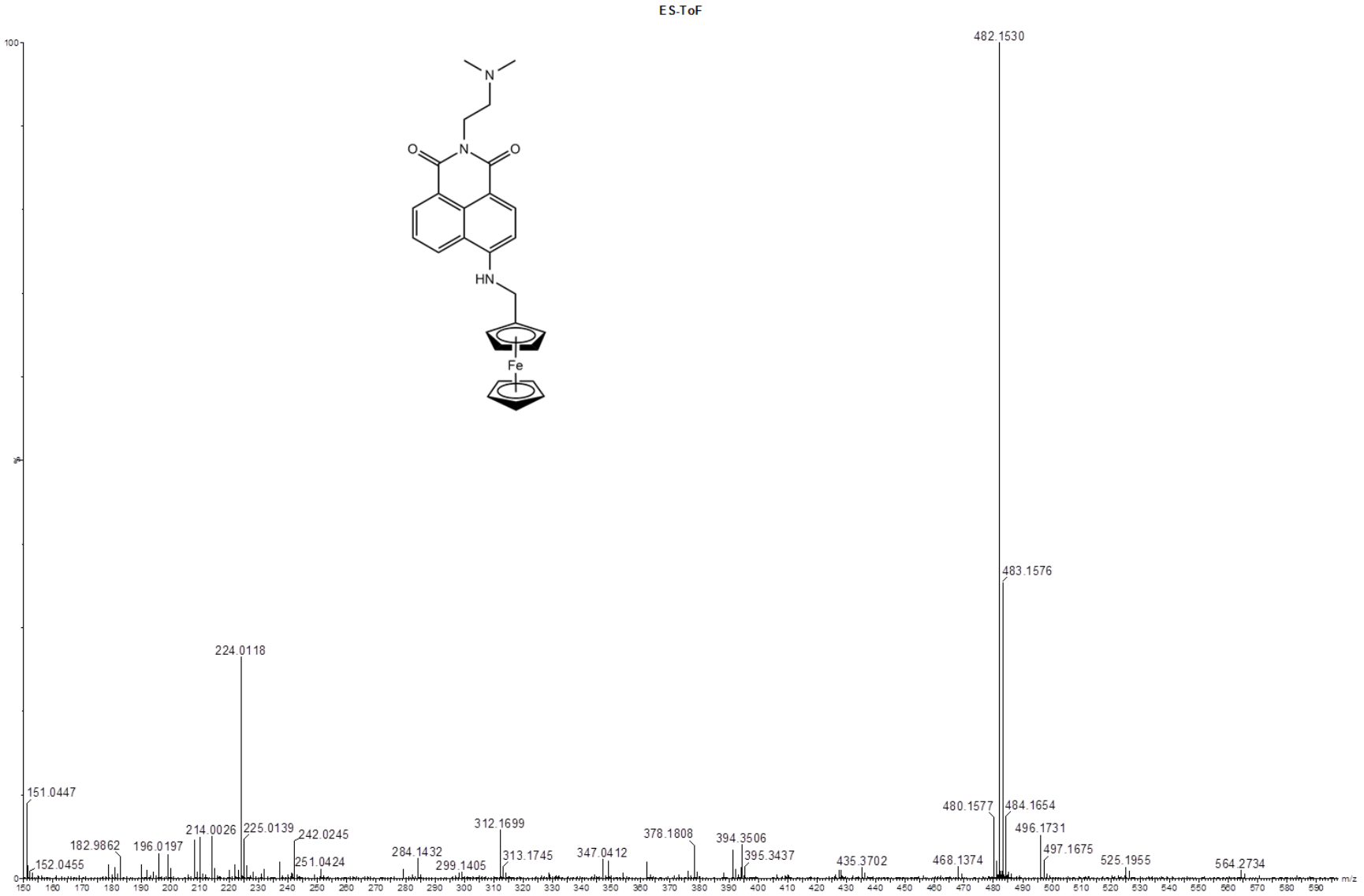

Fig. S15 High resolution MS of **2a** by electrospray time-of-flight mass technique.

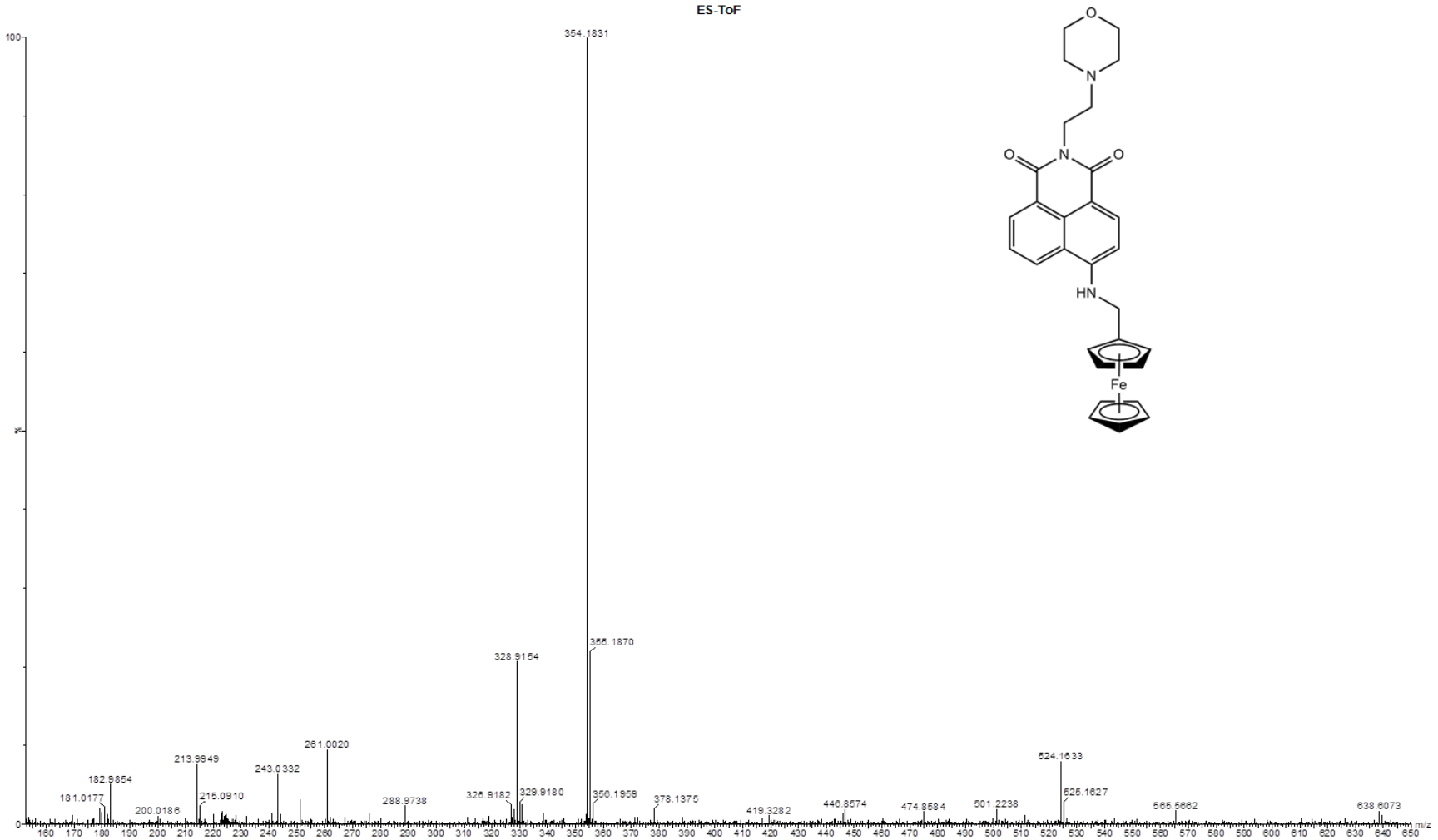

Fig. S16 High resolution MS of **2b** by electrospray time-of-flight mass technique.

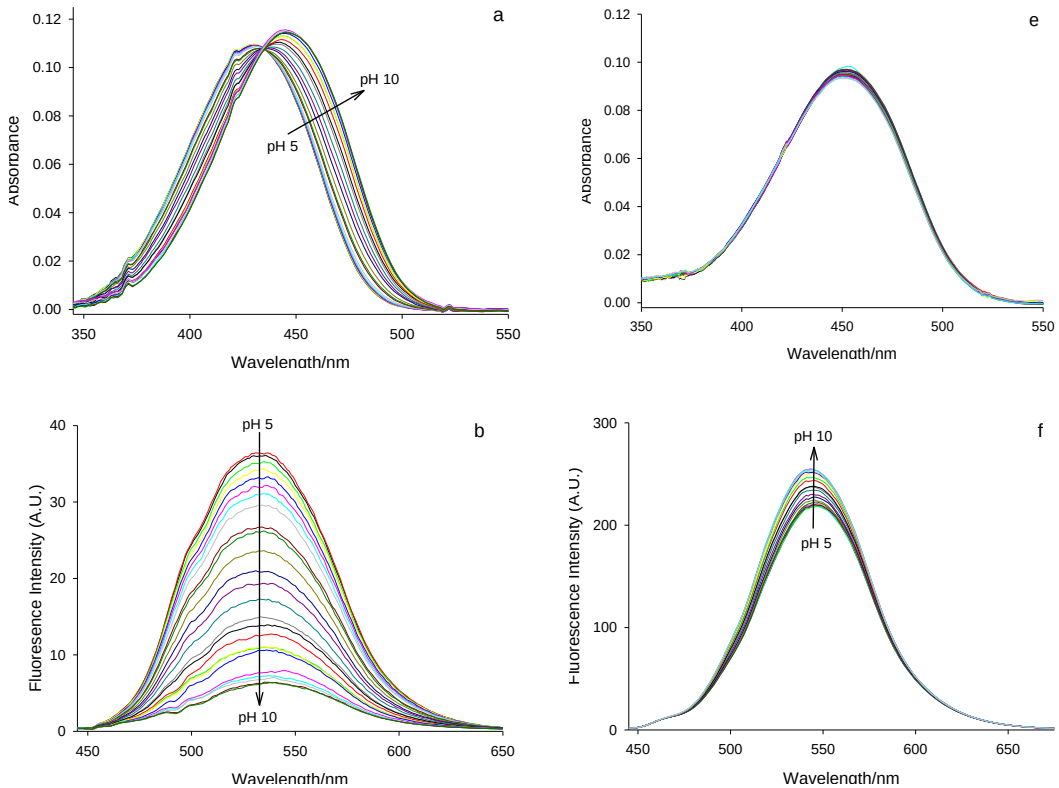

Fig. S17 pH titrations of 6.2 μM **1a** (a-b) and 8.2 μM **2a** (e-f) in 1:1 (*v*/*v*) MeOH/H_2O; (a/e) UV-Vis absorption spectra; (b/f) emission spectra.

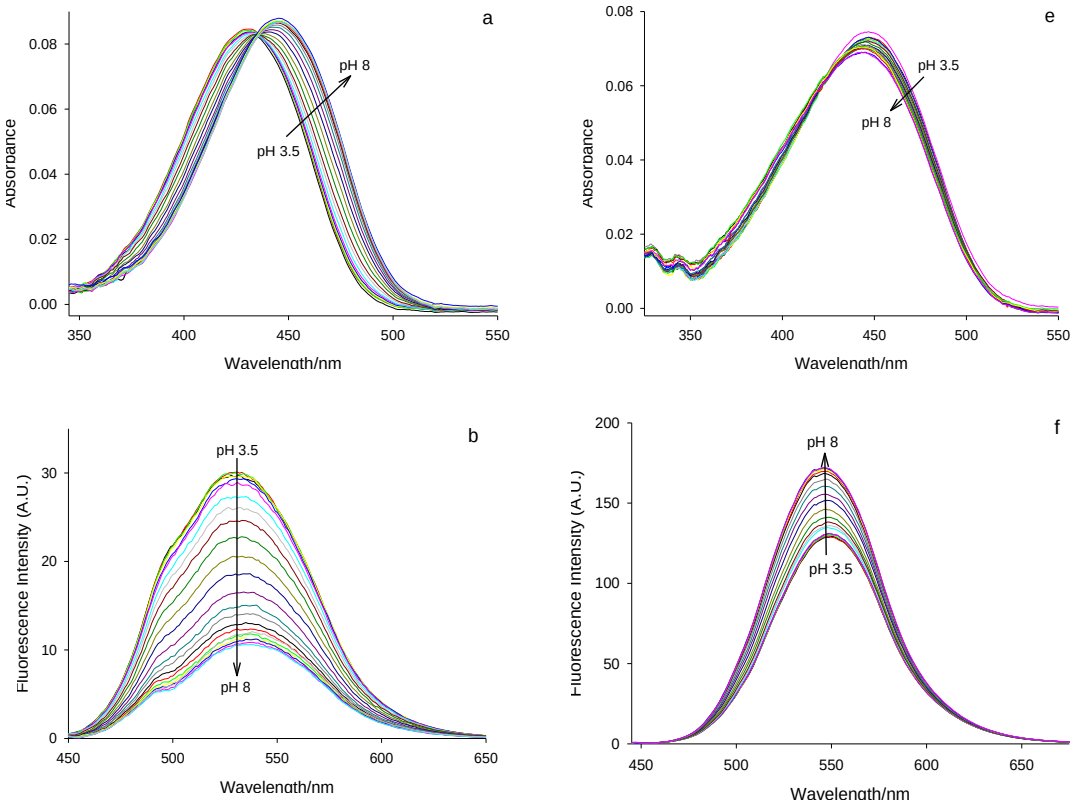

Fig. S18 pH titrations of 8.3 μM **1b** (a-e) and 8.0 μM **2b** (b-f) in 1:1 (*v*/*v*) MeOH/H_2O; (a/e) UV-Vis absorption spectra; (b/f) emission spectra.

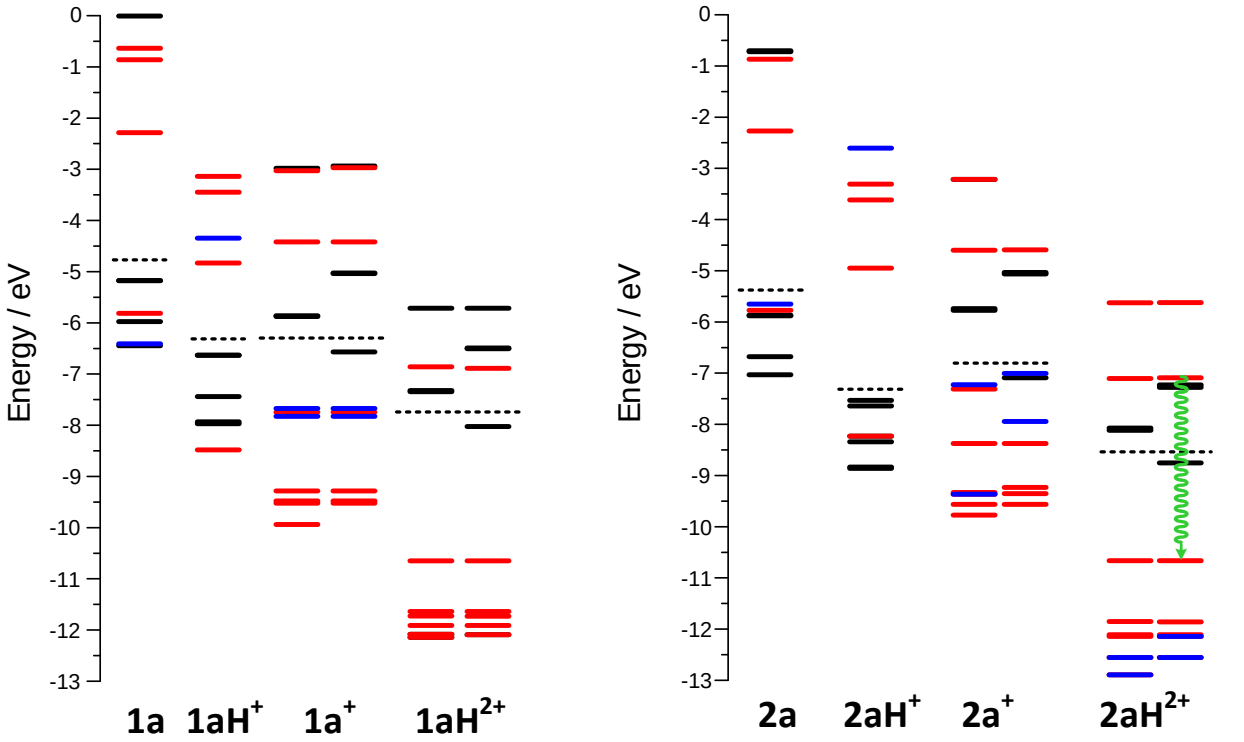

Fig. S19 Energy diagrams for neutral, protonated, oxidised, and protonated and oxidised forms of compounds **1a** and **2a** Energy levels associated with ferrocene/ferrocenium, amine and naphthalimide are shown in black, blue and red, respectively. The green arrows highlight transitions from ferrocenium-localised states.

1a	$1a^{+}$	$1aH^{+}$	$1aH^{2+}$
HOMO-5 -6.446 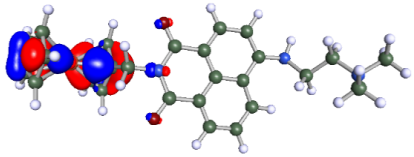	HOMO-5 (α) -9.938 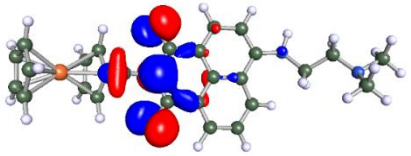 HOMO-5 (β) -9.521 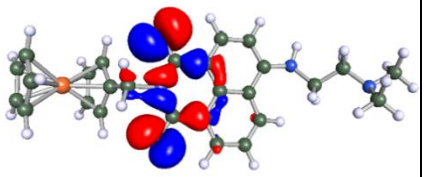	HOMO-5 -8.482 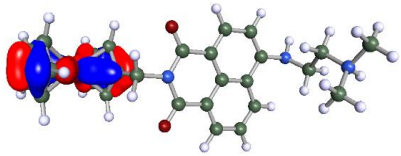	HOMO-5 (α) -12.144 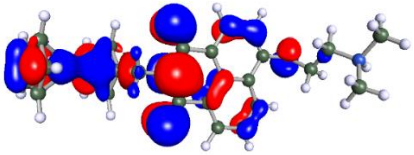 HOMO-5 (β) -12.090 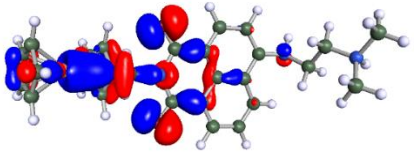
HOMO-4 -6.411 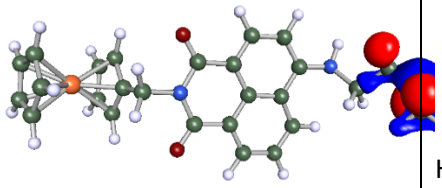	HOMO-4 (α) -9.521 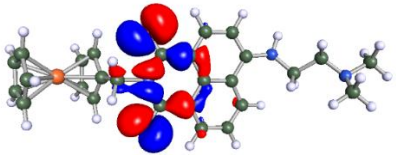 HOMO-4 (β) -9.480 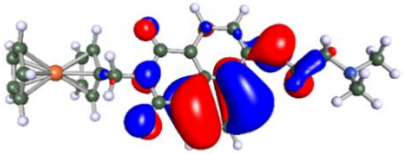	HOMO-4 -7.970 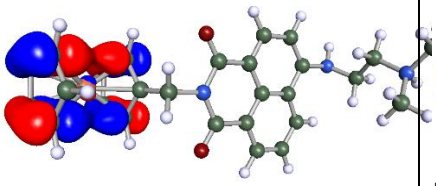	HOMO-4 (α) -12.082 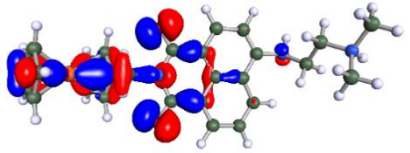 HOMO-4 (β) -11.910 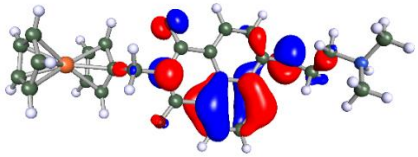
HOMO-3 -5.977 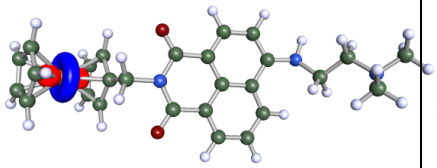	HOMO-3 (α) -9.480 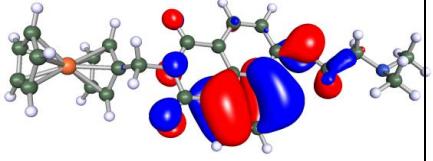	HOMO-3 -7.935 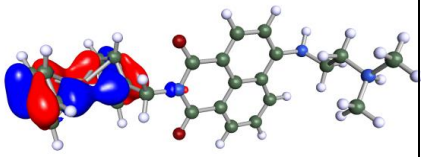	HOMO-3 (α) -11.910 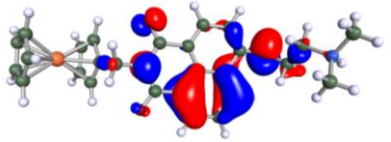

1a	$1a^{+}$	$1aH^{+}$	$1aH^{2+}$
	HOMO-3 (β) -9.285 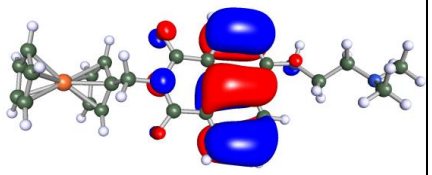		HOMO-3 (β) -11.728 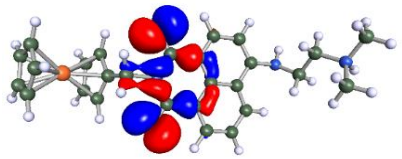
HOMO-2 -5.812 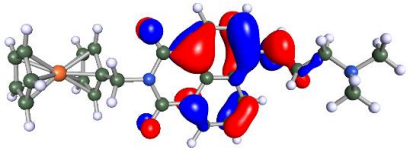	HOMO-2 (α) -9.285 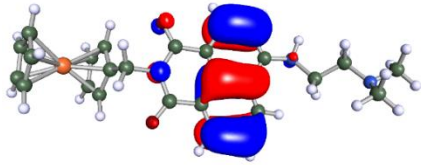 HOMO-2 (β) -7.826 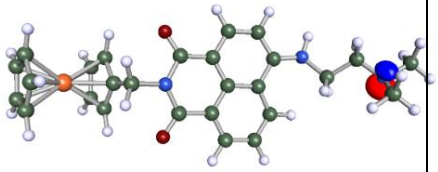	HOMO-2 -7.434 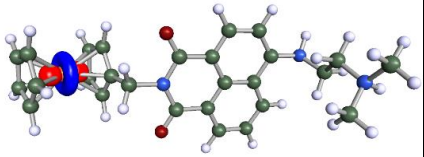	HOMO-2 (α) -11.728 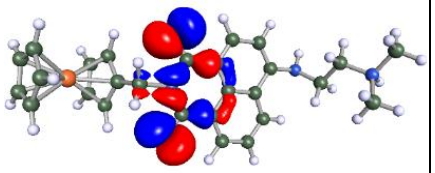 HOMO-2 (β) -11.640 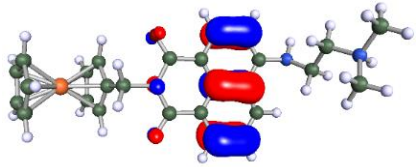
HOMO-1 -5.178 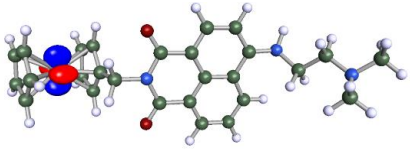	HOMO-1 (α) -7.826 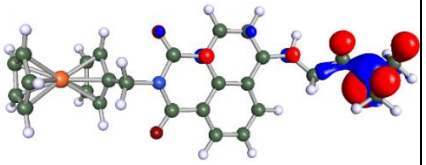 HOMO-1 (β) -7.747 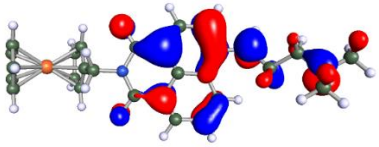	HOMO-1 -6.634 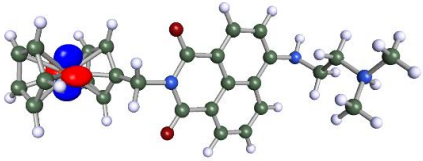	HOMO-1 (α) -11.640 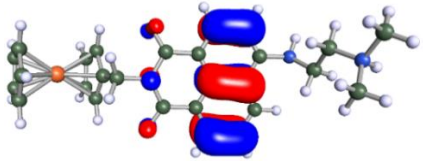 HOMO-1 (β) -10.651 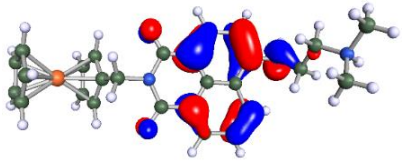

1a	$1a^{+}$	$1aH^{+}$	$1aH^{2+}$
HOMO -5.175 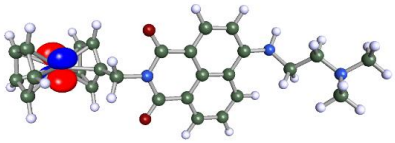	SOMO (α) -7.747 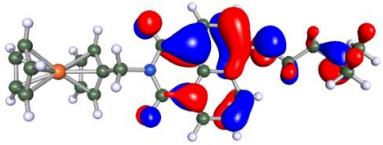 SOMO (β) -6.569 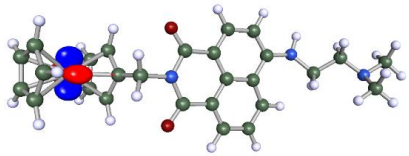	HOMO -6.629 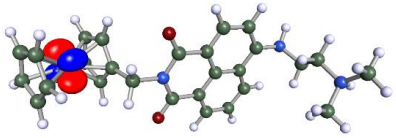	SOMO (α) -10.651 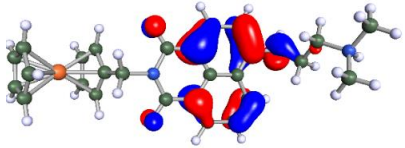 SOMO (β) -8.025 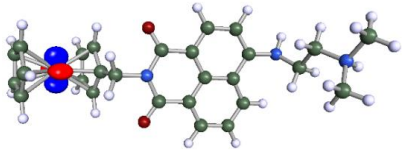
LUMO -2.284 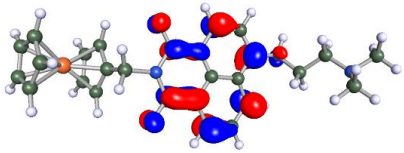	LUMO (α) -5.878 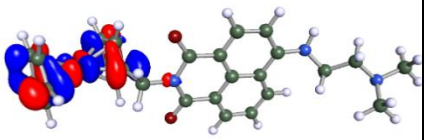 LUMO (β) -5.037 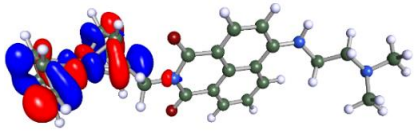	LUMO -4.830 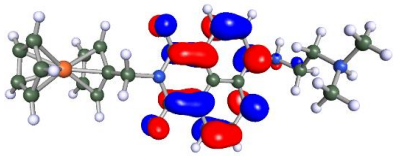	LUMO (α) -7.347 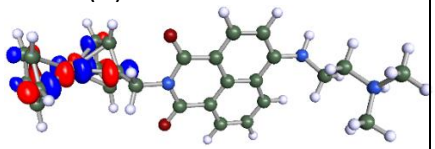 LUMO (β) -6.890 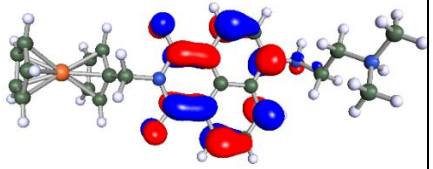
LUMO+1 -0.861 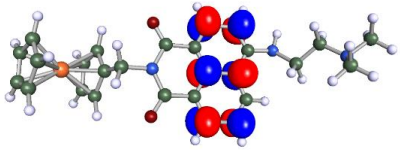	LUMO+1 (α) -5.859 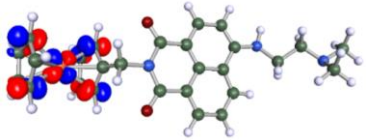 LUMO+1 (β) -5.026 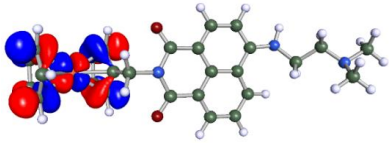	LUMO+1 -4.346 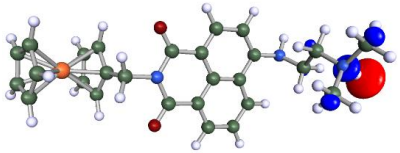	LUMO+1 (α) -7.323 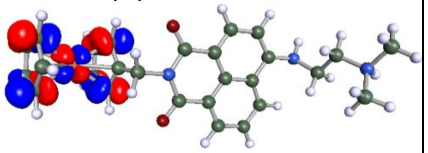 LUMO+1 (β) -6.504 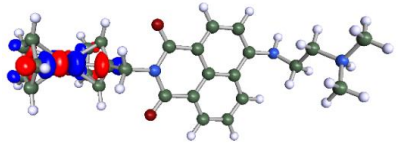

1a	**$1a^{+}$**	**$1aH^{+}$**	**$1aH^{2+}$**
LUMO+2 -0.636 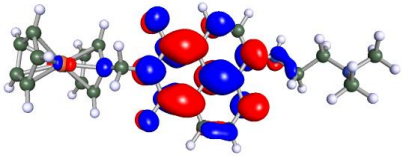	LUMO+2 (α) -4.419 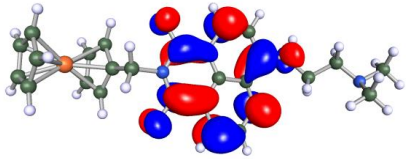 LUMO+2 (β) -4.416 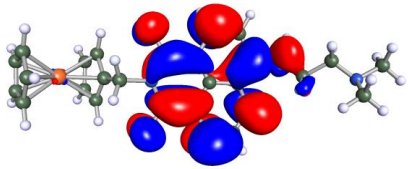	LUMO+2 -3.448 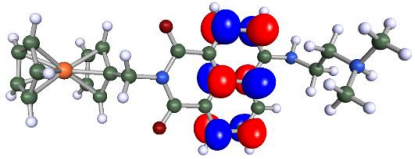	LUMO+2 (α) -6.887 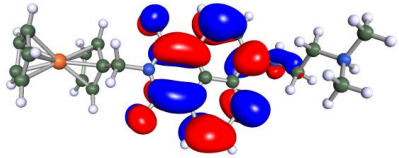 LUMO+2 (β) -6.490 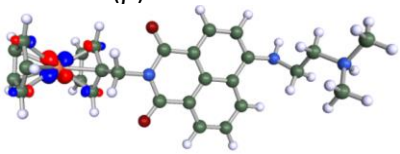
LUMO+3 -0.007 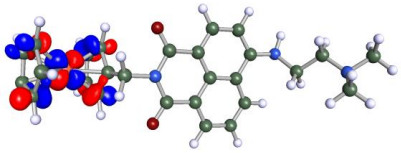	LUMO+3 (α) -2.980 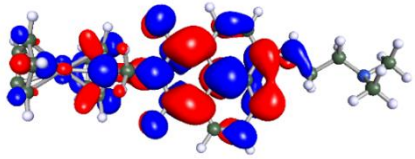 LUMO+3 (β) -2.963 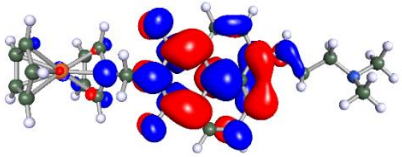	LUMO+3 -3.140 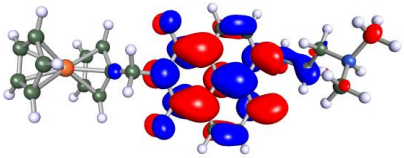	LUMO+3 (α) -5.714 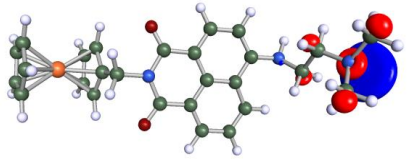 LUMO+3 (β) -5.714 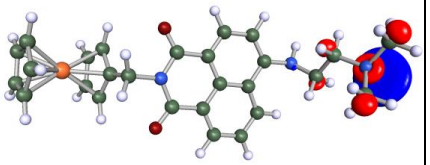

Fig. S20 Frontier orbitals of **1a** and its oxidized, protonated and oxidized protonated forms as calculated at the b3lyp/def2-TZVPP level of theory.

1b	$1b^{+}$	$1bH^{+}$	$1bH^{2+}$
HOMO-5 -6.544 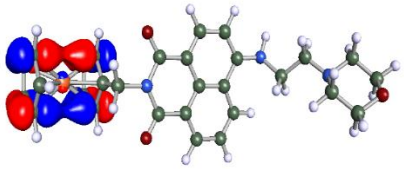	HOMO-5 (α) -9.548 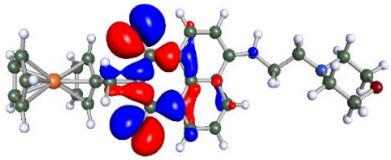 HOMO-5 (β) -9.516 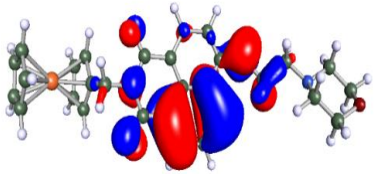	HOMO-5 -8.463 	HOMO-5 (α) -12.123 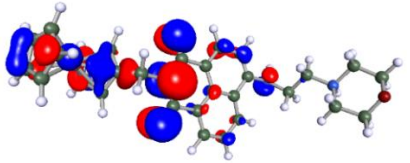 HOMO-5 (β) -12.071 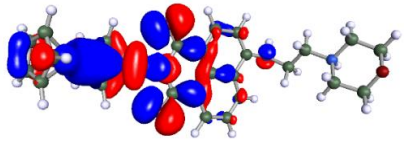
HOMO-4 -6.463 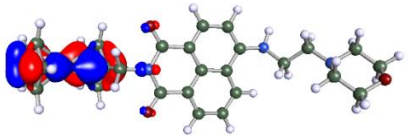	HOMO-4 (α) -9.516 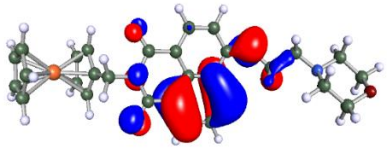 HOMO-4 (β) -9.317 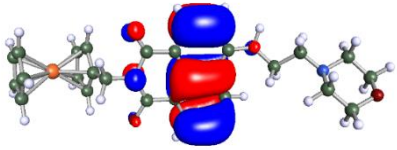	HOMO-4 -7.954 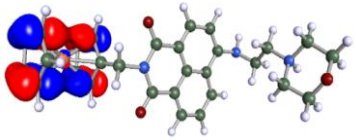	HOMO-4 (α) -12.063 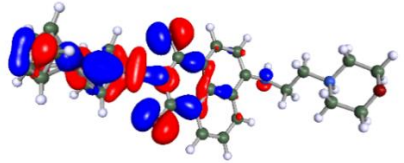 HOMO-4 (β) -11.872 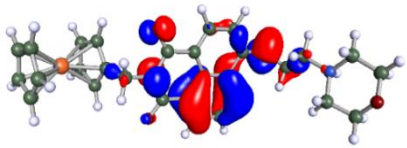
HOMO-3 -5.994 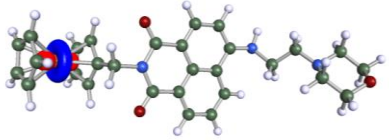	HOMO-3 (α) -9.317 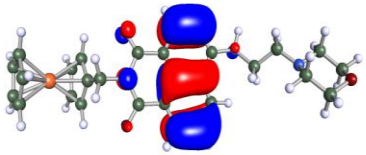	HOMO-3 -7.916 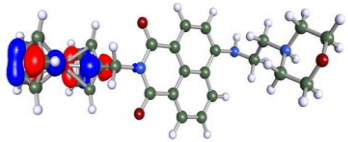	HOMO-3 (α) -11.872 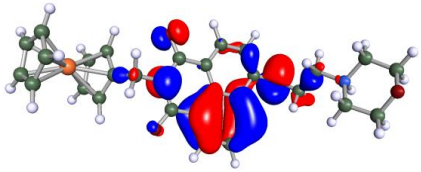

1b	$1b^{+}$	$1bH^{+}$	$1bH^{2+}$
	HOMO-3 (β) -8.618 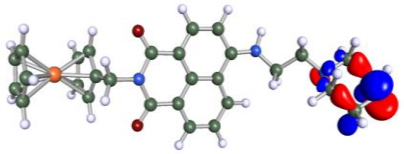		HOMO-3 (β) -11.706 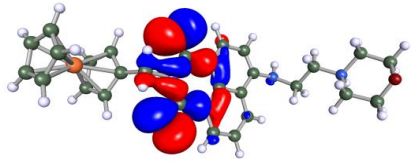
HOMO-2 -5.846 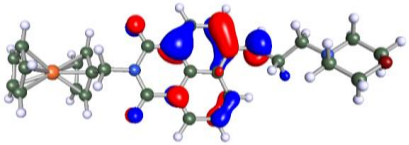	HOMO-2 (α) -8.618 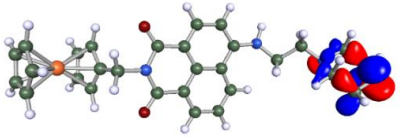 HOMO-2 (β) -7.935 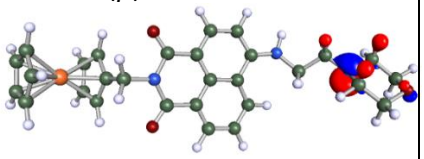	HOMO-2 -7.415 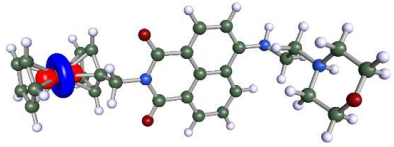	HOMO-2 (α) -11.706 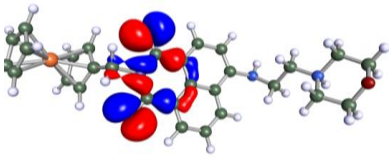 HOMO-2 (β) -11.614 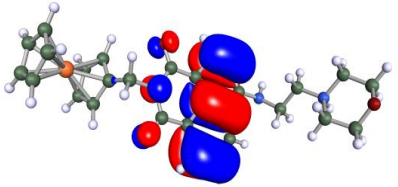
HOMO-1 -5.194 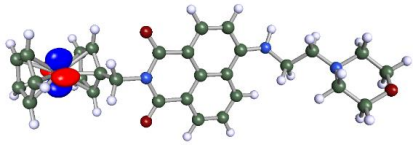	HOMO-1 (α) -7.935 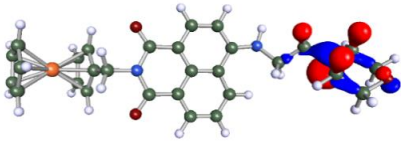 HOMO-1 (β) -7.791 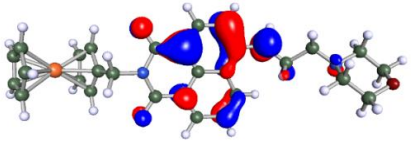	HOMO-1 -6.618 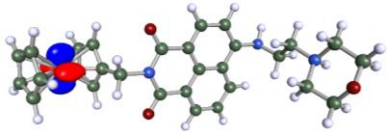	HOMO-1(α) -11.614 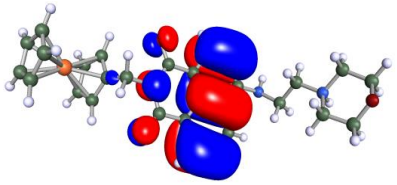 HOMO-1 (β) -10.618 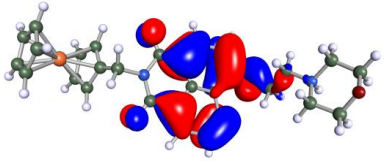

1b	$1b^{+}$	$1bH^{+}$	$1bH^{2+}$
HOMO -5.193 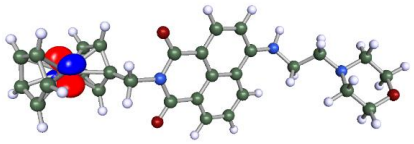	SOMO (α) -7.791 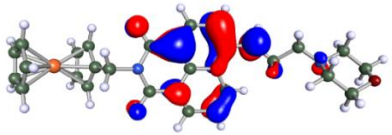 SOMO (β) -6.585 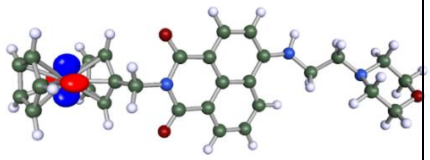	HOMO -6.612 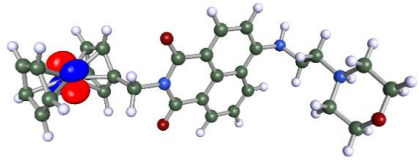	SOMO (α) -10.618 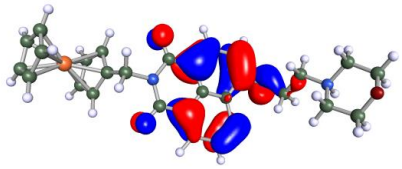 SOMO (β) -8.011 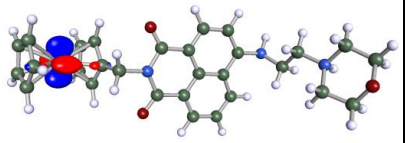
LUMO -2.315 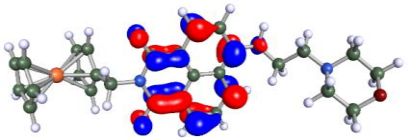	LUMO (α) -5.894 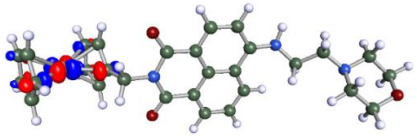 LUMO (β) -5.053 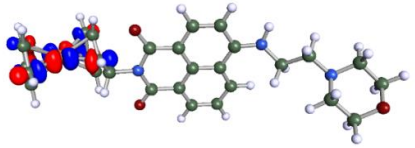	LUMO -4.792 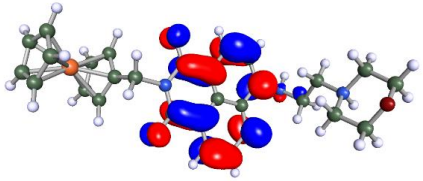	LUMO (α) -7.333 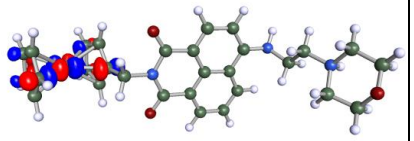 LUMO (β) -6.863 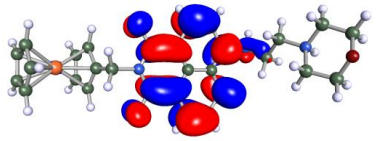
LUMO+1 -0.896 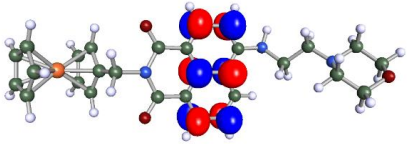	LUMO+1 (α) -5.878 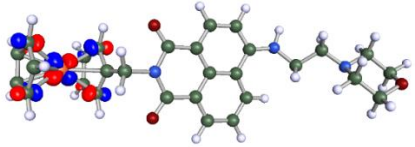 LUMO+1 (β) -5.042 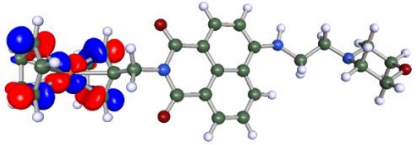	LUMO+1 -4.074 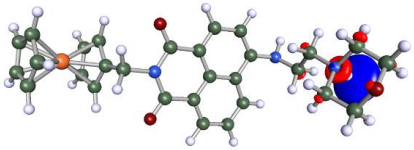	LUMO+1 (α) -7.312 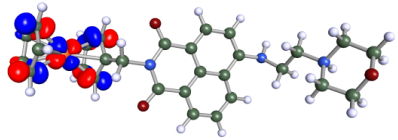 LUMO+1 (β) -6.493 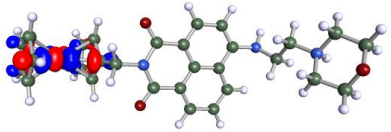

1b	1b^{+}	1bH^{+}	1bH^{2+}
LUMO+2 -0.669 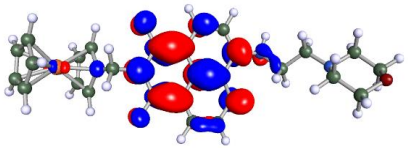	LUMO+2 (α) -4.446 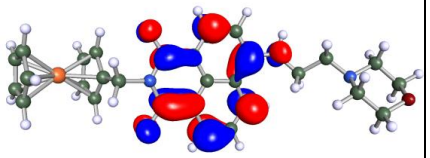 LUMO+2 (β) -4.446 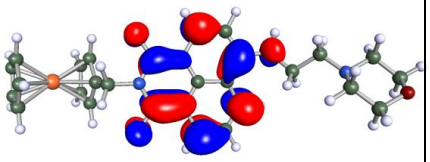	LUMO+2 -3.410 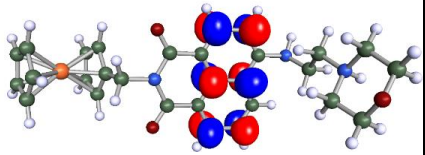	LUMO+2 (α) -6.860 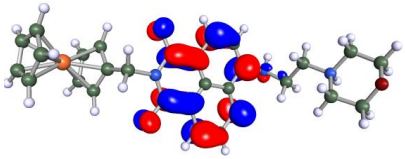 LUMO+2 (β) -6.476 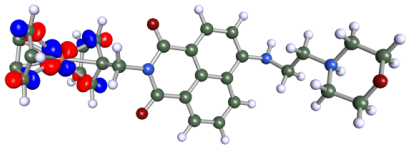
LUMO+3 -0.025 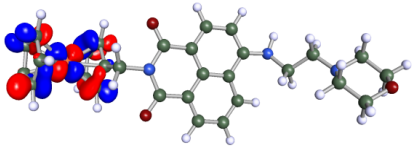	LUMO+3 (α) -3.007 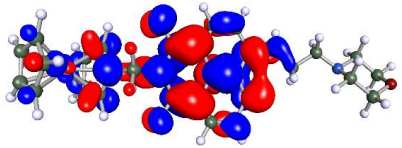 LUMO+3 (β) -2.993 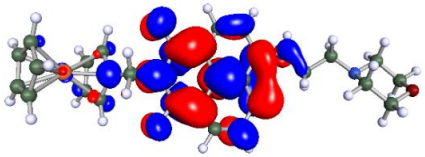	LUMO+3 -3.091 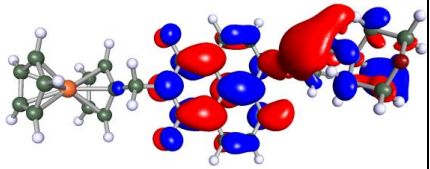	LUMO+3 (α) -5.437 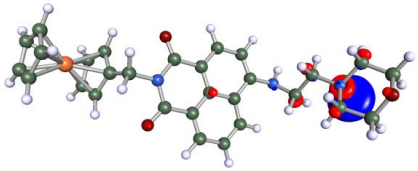 LUMO+3 (β) -5.437 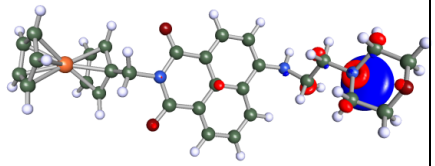

Fig. S21 Frontier orbitals of **1b** and its oxidized, protonated and oxidized protonated forms as calculated at the b3lyp/def2-TZVPP level of theory.

2a	$2a^{+}$	$2aH^{+}$	$2aH^{2+}$
HOMO-5 -7.031 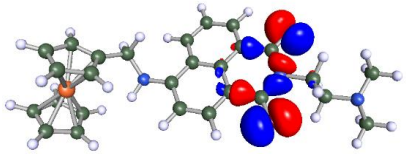	HOMO-5 (α) -9.774 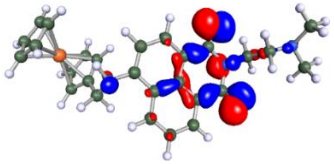 HOMO-5 (β) -9.562 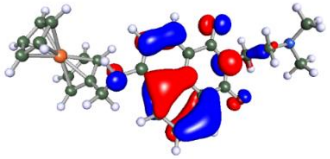	HOMO-5 -8.860 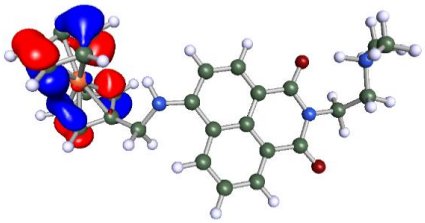	HOMO-5 (α) -12.895 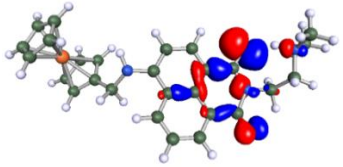 HOMO-5 (β) -12.555 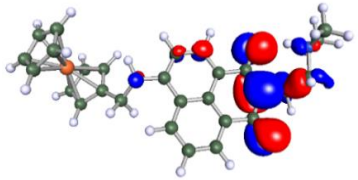
HOMO-4 -6.678 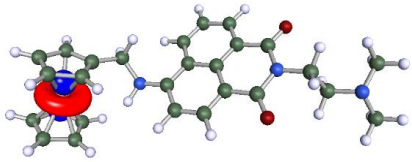	HOMO-4 (α) -9.565 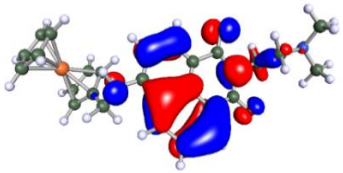 HOMO-4 (β) -9.355 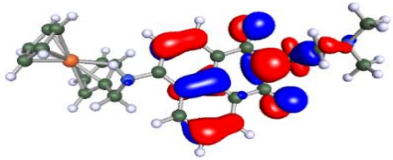	HOMO-4 -8.836 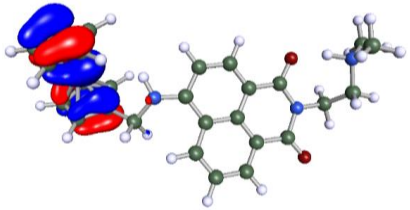	HOMO-4 (α) -12.555 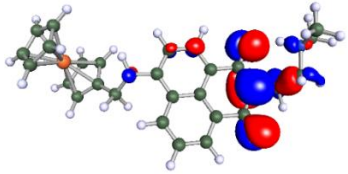 HOMO-4 (β) -12.144 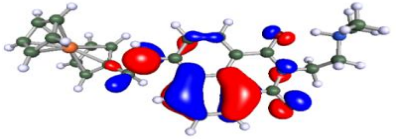
HOMO-3 -5.879 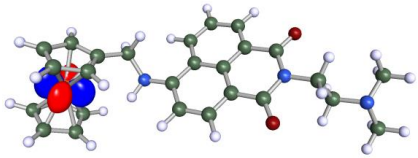	HOMO-3 (α) -9.363 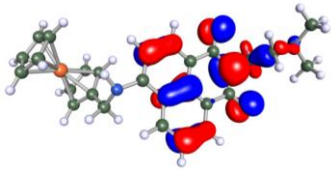	HOMO-3 -8.343 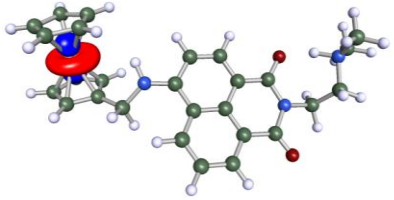	HOMO-3 (α) - 12.144 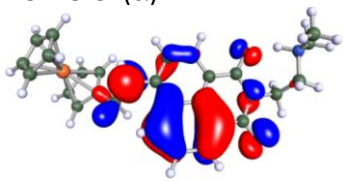

2a	$2a^{+}$	$2aH^{+}$	$2aH^{2+}$
	HOMO-3 (β) -9.233 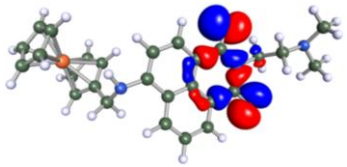		HOMO-3 (β) -12.111 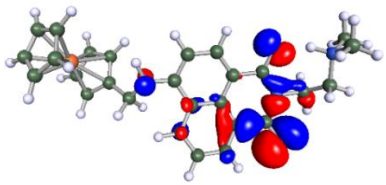
HOMO-2 -5.870 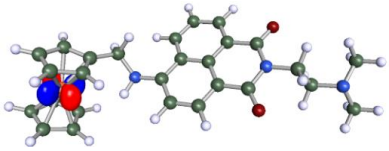	HOMO-2 (α) -9.233 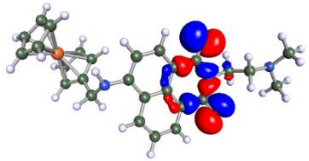 HOMO-2 (β) -8.376 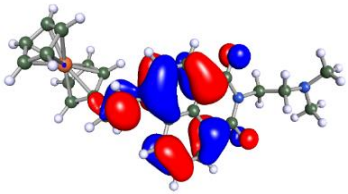	HOMO-2 -8.231 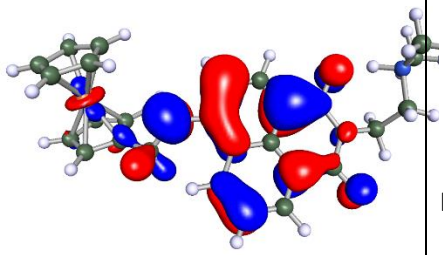	HOMO-2 (α) -12.111 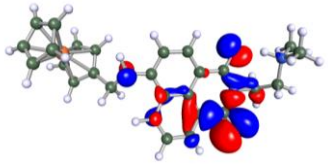 HOMO-2 (β) -11.853 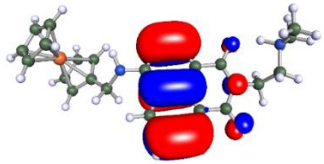
HOMO-1 -5.773 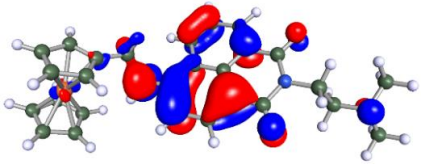	HOMO-1 (α) -8.376 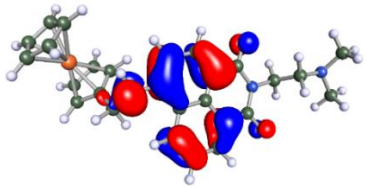 HOMO-1 (β) -7.943 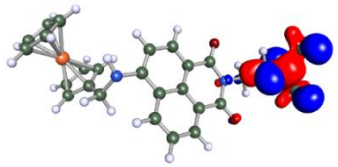	HOMO-1 -7.540 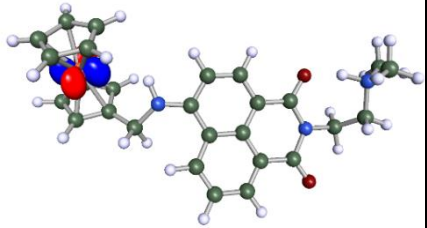	HOMO-1 (α) -11.853 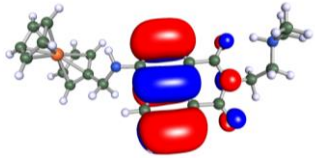 HOMO-1 (β) -10.664 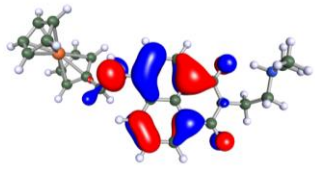

2a	$2a^{+}$	$2aH^{+}$	$2aH^{2+}$
HOMO -5.652 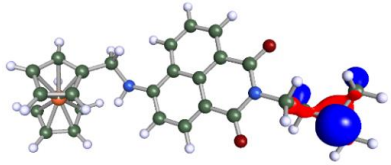	SOMO (α) -7.314 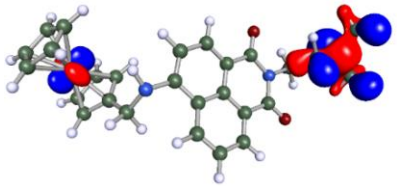 SOMO (β) -7.091 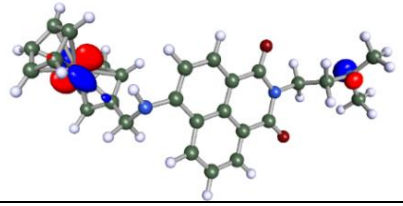	HOMO -7.532 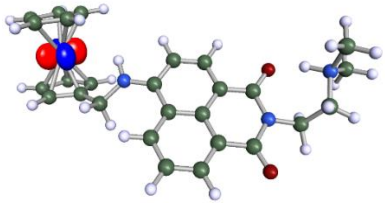	SOMO (α) -10.664 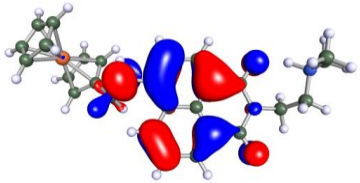 SOMO (β) -8.751 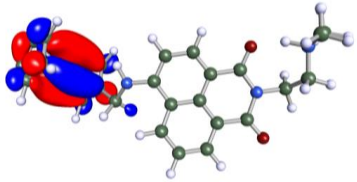
LUMO -2.272 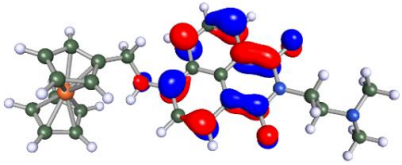	LUMO (α) -5.774 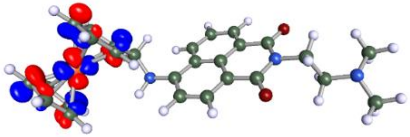 LUMO (β) -5.061 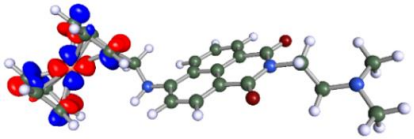	LUMO -4.947 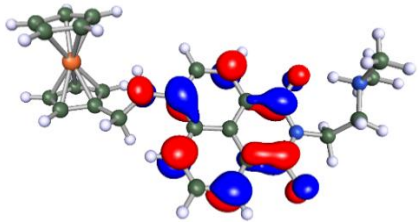	LUMO (α) -8.117 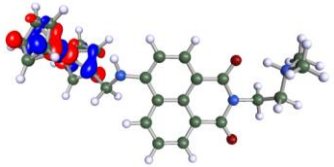 LUMO (β) -7.276 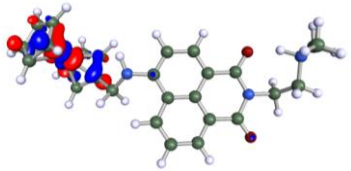
LUMO+1 -0.870 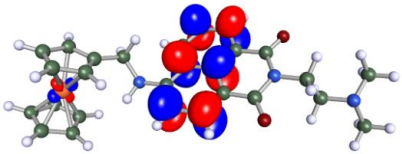	LUMO+1 (α) -5.739 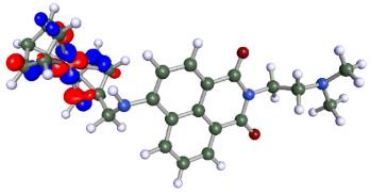	LUMO+1 -3.619 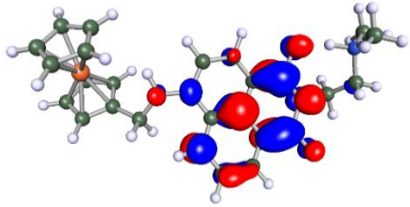	LUMO+1 (α) -8.074 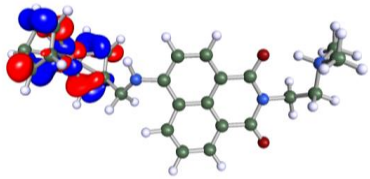

2a	$2a^{+}$	$2aH^{+}$	$2aH^{2+}$
	LUMO+1 (β) -5.031 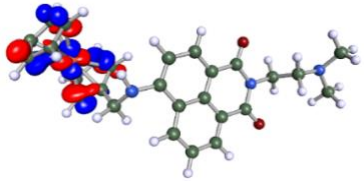		LUMO+1 (β) -7.230 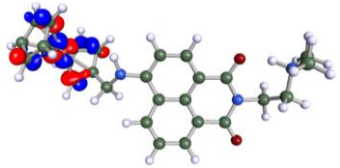
LUMO+2 -0.723 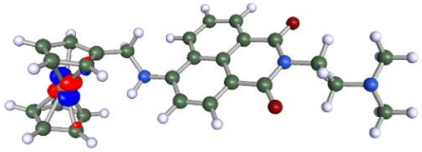	LUMO+2 (α) -4.601 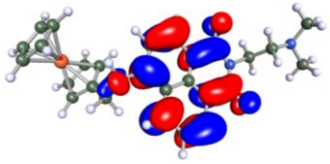 LUMO+2 (β) -4.593 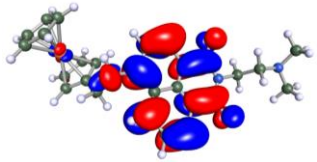	LUMO+2 -3.309 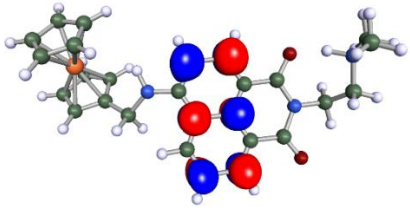	LUMO+2 (α) -7.105 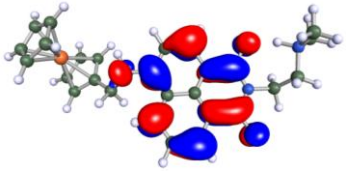 LUMO+2 (β) -7.089 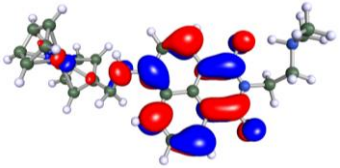
LUMO+3 -0.701 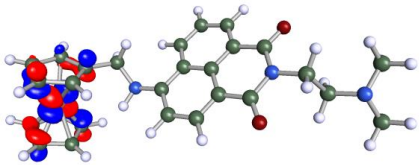	LUMO+3 (α) -3.216 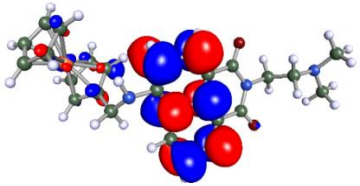 LUMO+3 (β) -3.206 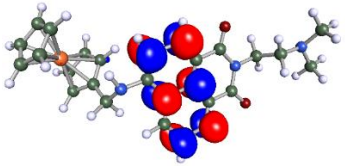	LUMO+3 -2.607 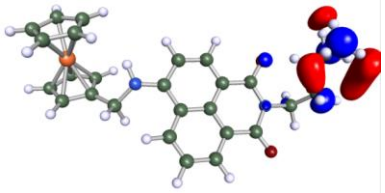	LUMO+3 (α) -5.627 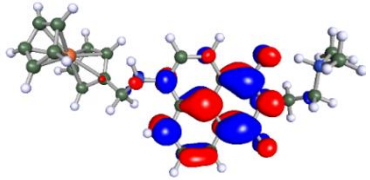 LUMO+3 (β) -5.622 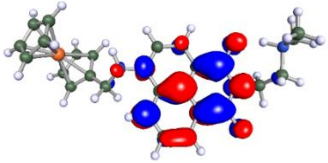

Fig. S22 Frontier orbitals of **2a** and its oxidized, protonated and oxidized protonated forms as calculated at the b3lyp/def2-TZVPP level of theory.

2b	$2b^{+}$	$2bH^{+}$	$2bH^{2+}$
HOMO-5 -6.816 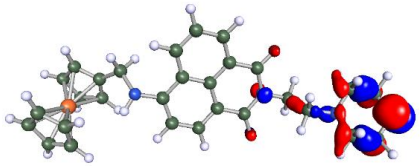	HOMO-5 (α) -9.587 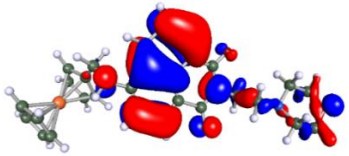 HOMO-5 (β) -9.344 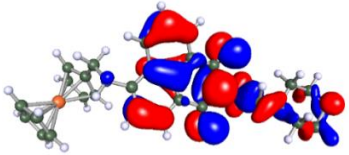	HOMO-5 -8.876 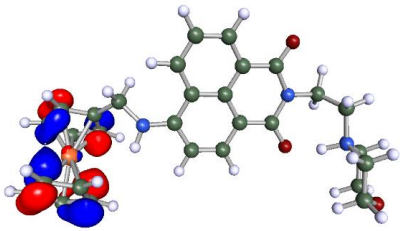	HOMO-5 (α) -12.321 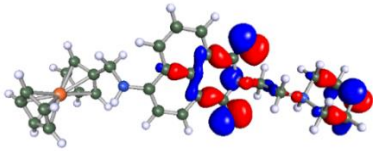 HOMO-5 (β) -12.134 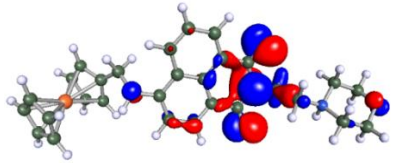
HOMO-4 -6.702 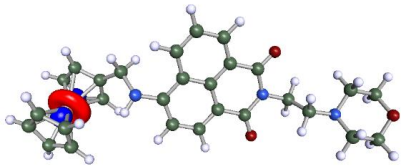	HOMO-4 (α) -9.350 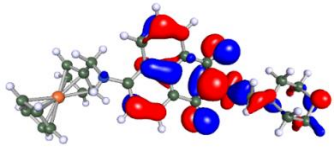 HOMO-4 (β) -9.225 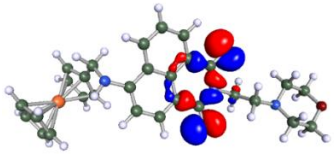	HOMO-4 -8.849 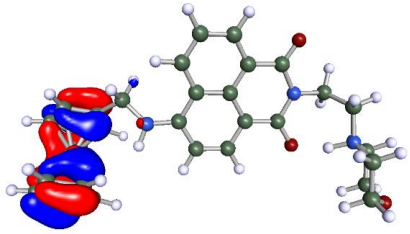	HOMO-4 (α) -12.131 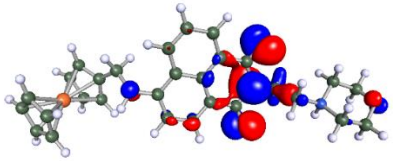 HOMO-4 (β) -11.834 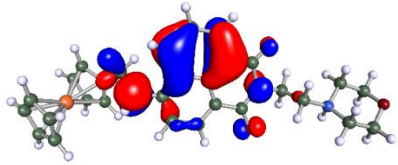
HOMO-3 -5.903 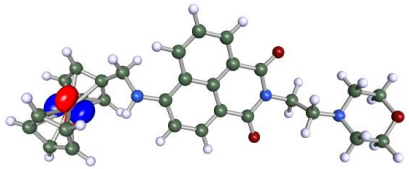	HOMO-3 (α) -9.225 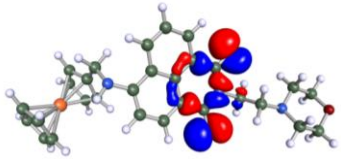	HOMO-3 -8.357 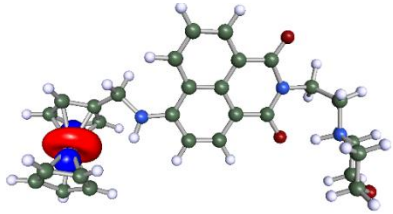	HOMO-3 (α) -11.834 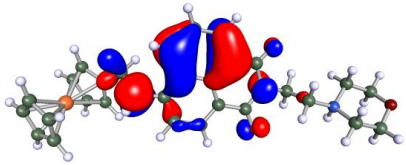

2b	$2b^{+}$	$2bH^{+}$	$2bH^{2+}$
	HOMO-3 (β) -8.436 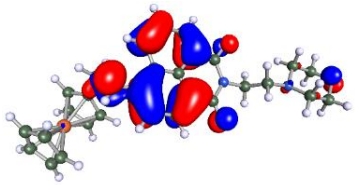		HOMO-3 (β) -11.715 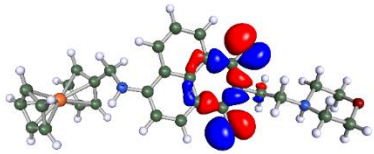
HOMO-2 -5.893 	HOMO-2 (α) -8.444 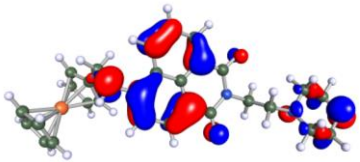 HOMO-2 (β) -8.389 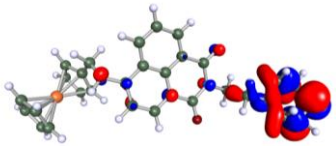	HOMO-2 -8.231 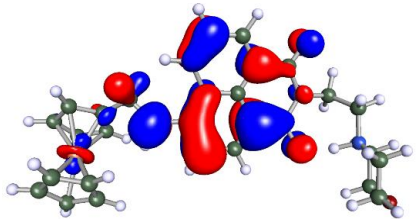	HOMO-2 (α) -11.715 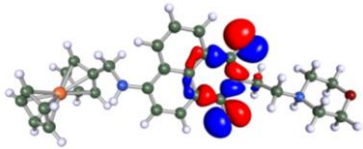 HOMO-2 (β) -11.551 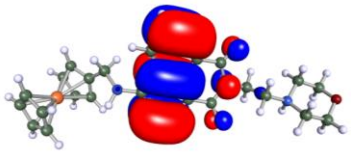
HOMO-1 -5.850 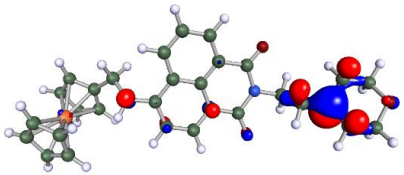	HOMO-1 (α) -8.414 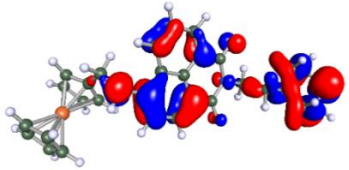 HOMO-1 (β) -7.684 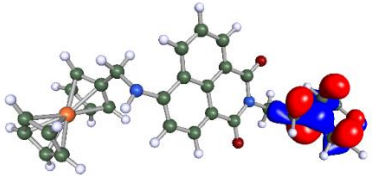	HOMO-1 -7.554 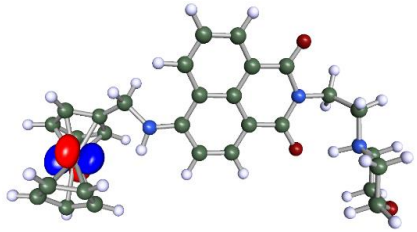	HOMO-1 (α) -11.551 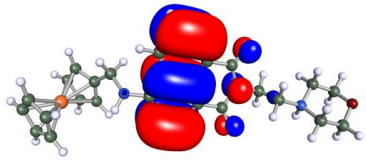 HOMO-1 (β) -10.384 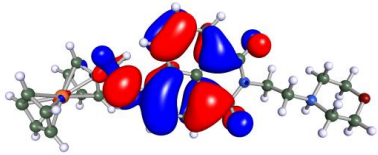

2b	$2b^{+}$	$2bH^{+}$	$2bH^{2+}$
HOMO -5.796 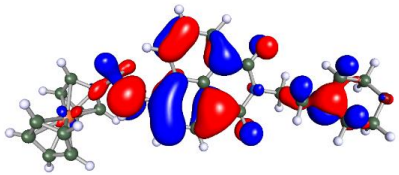	SOMO (α) -7.355 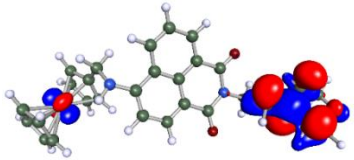 SOMO (β) -7.132 	HOMO -7.546 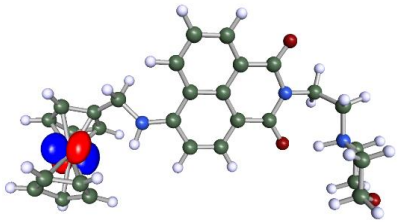	SOMO (α) -10.381 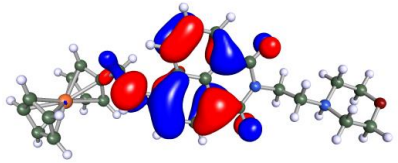 SOMO (β) -8.566 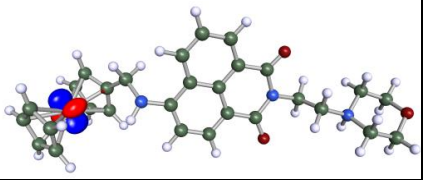
LUMO -2.319 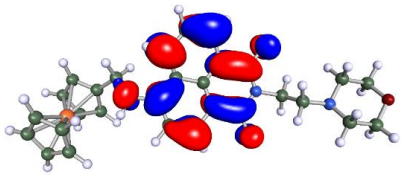	LUMO (α) -6.098 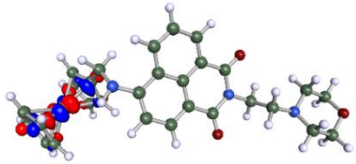 LUMO (β) -5.328 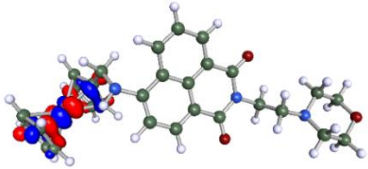	LUMO -4.944 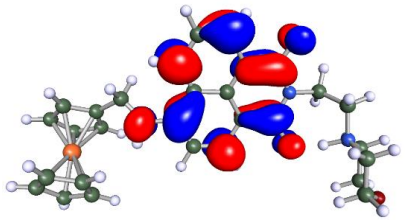	LUMO (α) -7.929 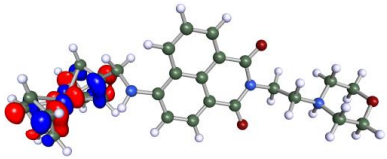 LUMO (β) -7.083 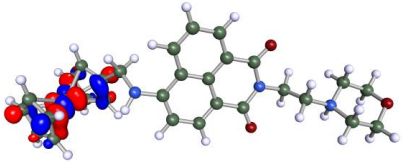
LUMO+1 -0.912 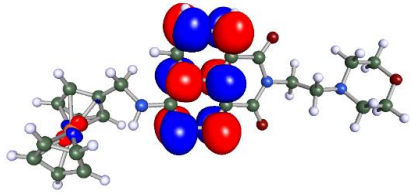	LUMO+1 (α) -6.063 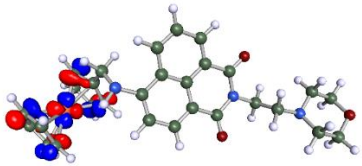 LUMO+1 (β) -5.298	LUMO+1 -3.606 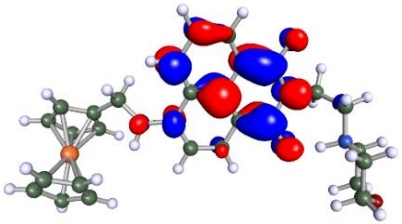	LUMO+1 (α) -7.886 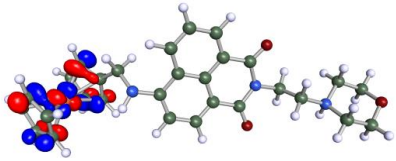 LUMO+1 (β) -7.042

2b	$2b^{+}$	$2bH^{+}$	$2bH^{2+}$
	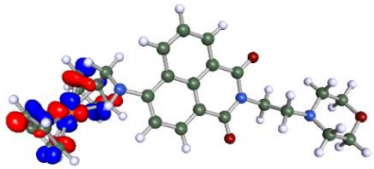		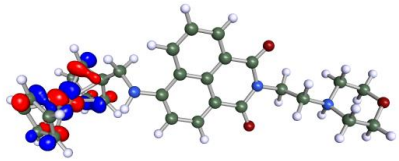
LUMO+2 -0.749 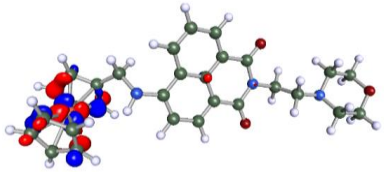	LUMO+2 (α) -4.637 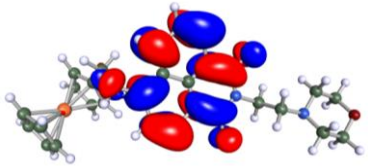 LUMO+2 (β) -4.631 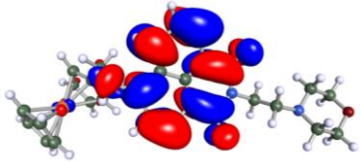	LUMO+2 -3.312 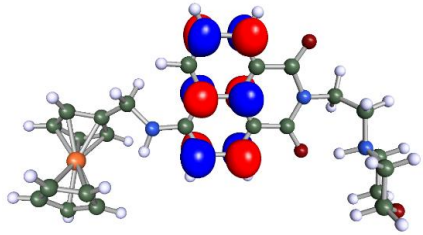	LUMO+2 (α) -6.754 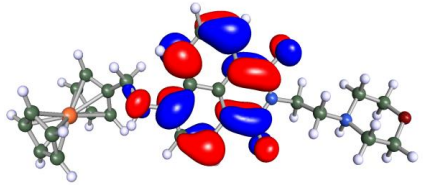 LUMO+2 (β) -6.746 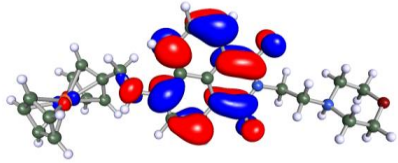
LUMO+3 -0.726 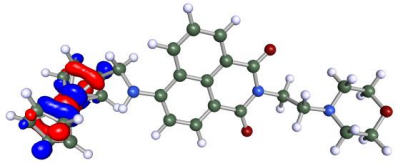	LUMO+3 (α) -3.293 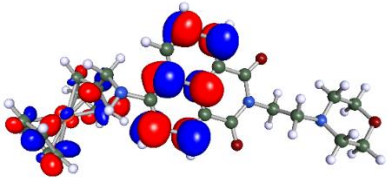 LUMO+3 (β) -3.263 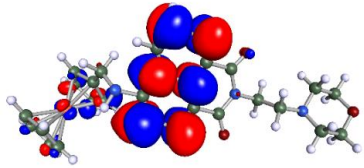	LUMO+3 -2.512 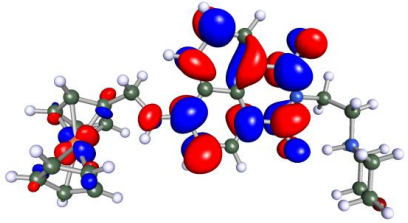	LUMO+3 (α) -5.244 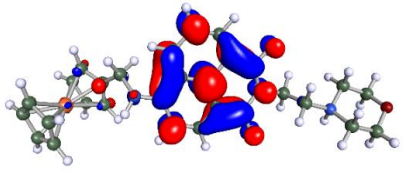 LUMO+3 (β) -5.233 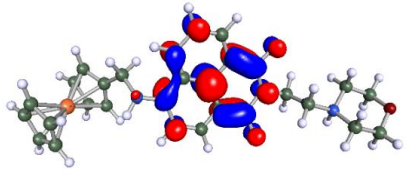

Fig. S23 Frontier orbitals of **2b** and its oxidized, protonated and oxidized protonated forms as calculated at the b3lyp/def2-TZVPP level of theory.

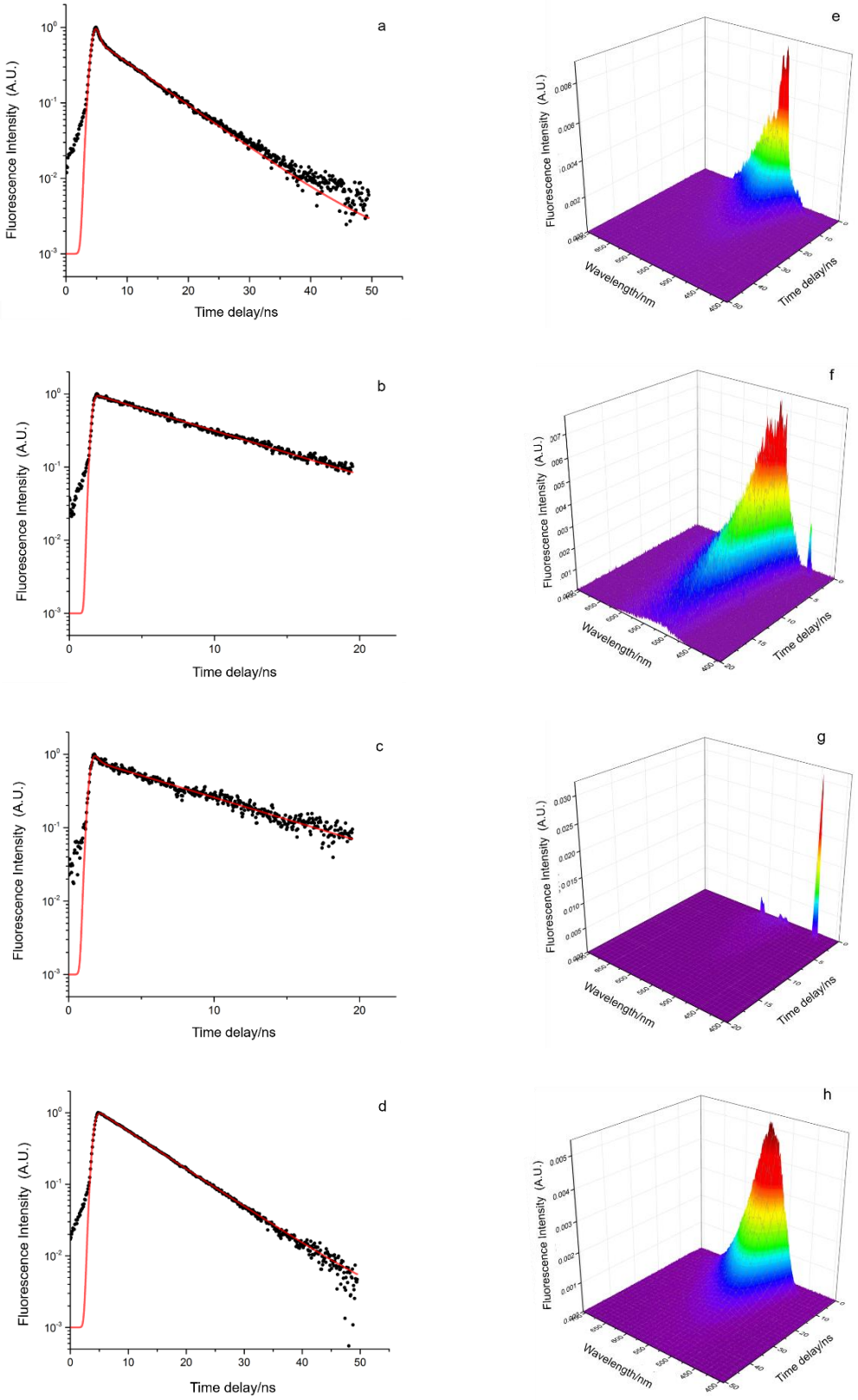

Fig. S24 Fluorescence decay curves (a-d) and 3D surface plots (e-h) of **1a** in 1:1 (*v*/*v*) MeOH/H_2O; (a/e) pH 9, (b/f) pH 4, (c/g) pH 9 with 50 μM Fe^{3+} (d/h) pH 4 with 50 μM Fe^{3+}.

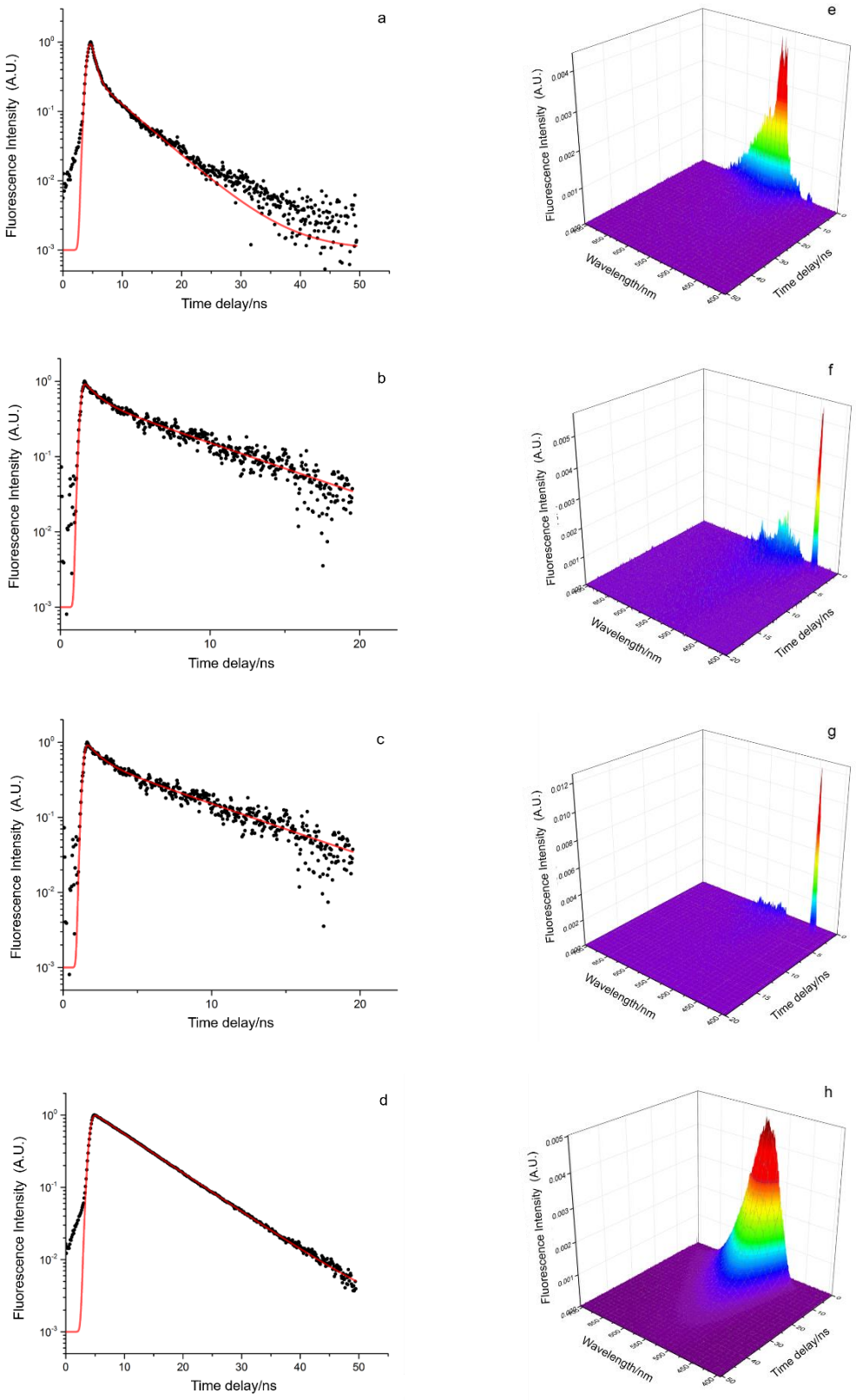

Fig. S25 Fluorescence decay curves (a-d) and 3D surface plots (e-h) of **1b** in 1:*1 (v/v)* MeOH/H_2O; (a/e) pH 9, (b/f) pH 4, (c/g) pH 9 with 50 μM Fe^{3+} (d/h) pH 4 with 50 μM Fe^{3+}.

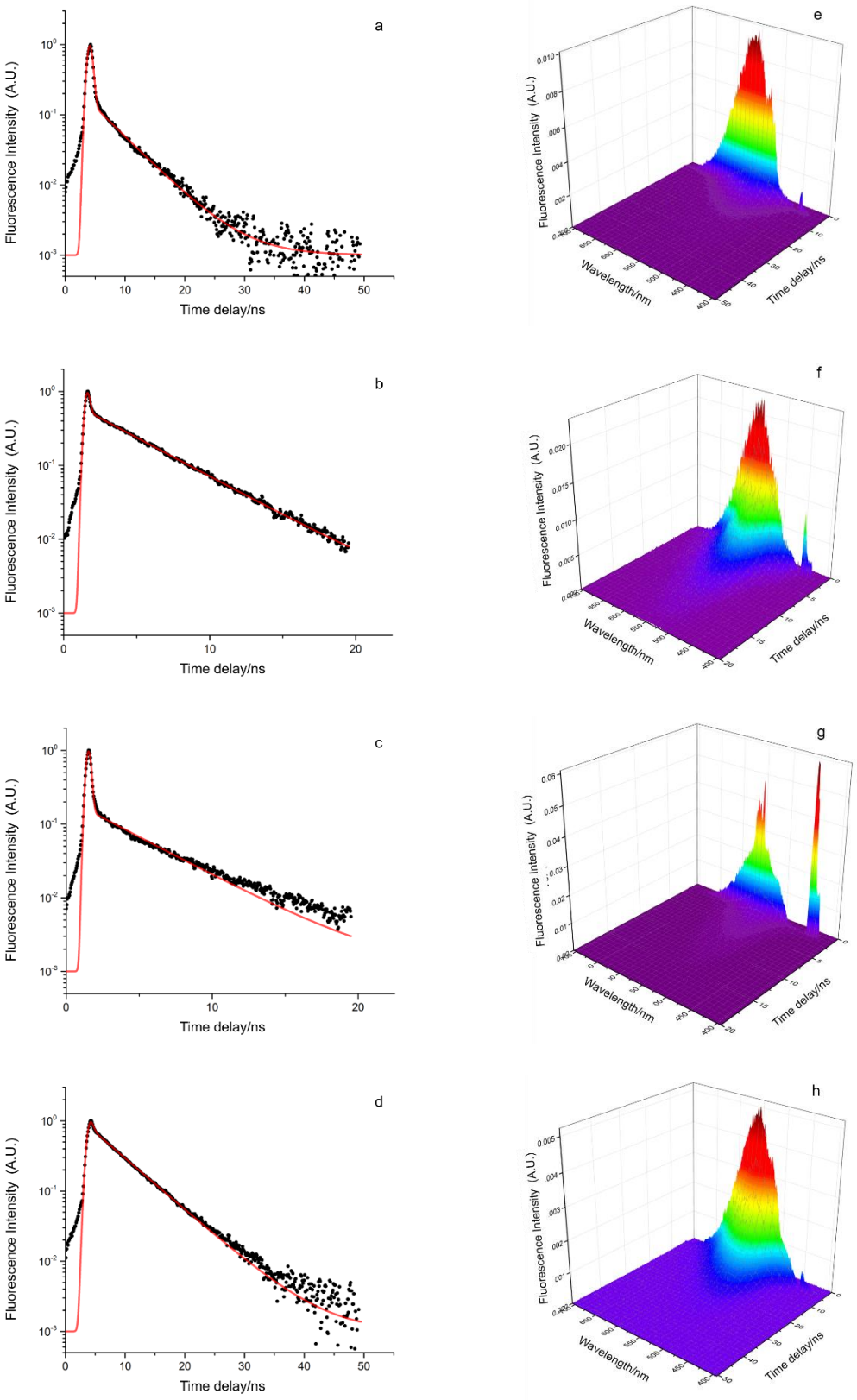

Fig. S26 Fluorescence decay curves (a-d) and 3D surface plots (e-h) of **2b** in 1:1 (*v*/*v*) MeOH/H_2O; (a/e) pH 9, (b/f) pH 4, (c/g) pH 9 with 50 μM Fe^{3+} (d/h) pH 4 with 50 μM Fe^{3+}.